

EFFECT OF THIRD METAL ON THE PERFORMANCE OF Pt/WO_x/Al₂O₃ FOR
HYDROGENOLYSIS OF GLYCEROL



A Thesis Submitted in Partial Fulfillment of the Requirements
for the Degree of Master of Engineering in Chemical Engineering

Department of Chemical Engineering

FACULTY OF ENGINEERING

Chulalongkorn University

Academic Year 2020

Copyright of Chulalongkorn University

ผลกระทบบของโลหะตัวที่สามบน Pt/WO_x/Al₂O₃ ต่อประสิทธิภาพสำหรับปฏิกิริยาไฮโดรจีโนไลซิสของ
กลีเซอรอล



วิทยานิพนธ์นี้เป็นส่วนหนึ่งของการศึกษาตามหลักสูตรปริญญาวิศวกรรมศาสตรมหาบัณฑิต
สาขาวิชาวิศวกรรมเคมี ภาควิชาวิศวกรรมเคมี
คณะวิศวกรรมศาสตร์ จุฬาลงกรณ์มหาวิทยาลัย
ปีการศึกษา 2563
ลิขสิทธิ์ของจุฬาลงกรณ์มหาวิทยาลัย

Thesis Title	EFFECT OF THIRD METAL ON THE PERFORMANCE OF Pt/WO _x /Al ₂ O ₃ FOR HYDROGENOLYSIS OF GLYCEROL
By	Mr. Therasak Tapanya
Field of Study	Chemical Engineering
Thesis Advisor	Professor PIYASAN PRASERTHDAM, Dr.Ing.
Thesis Co Advisor	Dr. SUPAREAK PRASERTHDAM, Ph.D.

Accepted by the FACULTY OF ENGINEERING, Chulalongkorn University in
Partial Fulfillment of the Requirement for the Master of Engineering

..... Dean of the FACULTY OF
ENGINEERING
(Professor SUPOT TEACHAVORASINSKUN, D.Eng.)

THESIS COMMITTEE

..... Chairman
(Assistant Professor AMORNCHAI ARPORNWICHANOP,
D.Eng.)

..... Thesis Advisor
(Professor PIYASAN PRASERTHDAM, Dr.Ing.)

..... Thesis Co-Advisor
(Dr. SUPAREAK PRASERTHDAM, Ph.D.)

..... Examiner
(Assistant Professor SUPHOT PHATANASRI, D.Eng.)

..... External Examiner
(Associate Professor Okorn Mekasuwandumrong, D.Eng.)

ธีรศักดิ์ ทาปัญญา : ผลกระทบของโลหะตัวที่สามบน Pt/WO_x/Al₂O₃ ต่อประสิทธิภาพ
 สำหรับปฏิกิริยาไฮโดรจิโนไลซิสของกลีเซอรอล. (EFFECT OF THIRD METAL ON
 THE PERFORMANCE OF Pt/WO_x/Al₂O₃ FOR HYDROGENOLYSIS OF
 GLYCEROL) อ.ที่ปรึกษาหลัก : ศ. ดร.ปิยะสาร ประเสริฐธรรม, อ.ที่ปรึกษาร่วม : ดร.ศุภ
 ฤกษ์ ประเสริฐธรรม

ปฏิกิริยาไฮโดรจิโนไลซิสใช้เพื่อเปลี่ยนกลีเซอรอลเป็นสารเคมีที่มีค่า โดยเฉพาะ 1,3-โพรเพนไดออล ในการศึกษาี้ ประสิทธิภาพ ซึ่งรวมถึงความสามารถในการเปลี่ยนแปลงกลีเซอรอล ค่าการเลือกเกิด และความเสถียรภาพ สำหรับตัวเร่งปฏิกิริยาแพลทินัม-ทังสเทนออกไซด์บนอะลูมินา ที่ถูกพัฒนาด้วยโลหะที่สาม ตัวเร่งปฏิกิริยาถูกเตรียมโดยใช้วิธีการเคลือบฝังแบบเปียกและเปียกพอดี โดยการศึกษาคุณสมบัติทางสัณฐานวิทยาของตัวเร่งปฏิกิริยาด้วยเทคนิค ภาพถ่ายทางสัณฐานวิทยา การดูดซับทางกายภาพด้วยไนโตรเจน การดูดซับทางเคมีด้วยคาร์บอนมอนอกไซด์ ความเสถียรภาพของตัวเร่งปฏิกิริยาได้รับการทดสอบผ่านปฏิกิริยาไฮโดรจิโนไลซิสรอบที่สอง ซึ่งศึกษาผลการเสื่อมสภาพโดยการวิเคราะห์ การเลี้ยวเบนของรังสีเอ็กซ์ อินดักทีฟพลาสมา และเทคนิคโปรแกรมอุณหภูมิเพื่อทดสอบการออกซิเดชัน ผลการวิจัยพบว่าการเพิ่มโลหะที่สามบนตัวเร่งปฏิกิริยาแพลทินัม-ทังสเทนออกไซด์บนอะลูมินา ช่วยเพิ่มค่าการเปลี่ยนแปลงกลีเซอรอล ในขณะที่ รีเนียม โรเดียม และซิลิโคทังสติก แสดงให้เห็นถึงความเสถียรภาพที่ดีขึ้น อย่างไรก็ตาม รีเนียม โรเดียม และซิลิโคทังสติก สามารถปรับปรุงการเสื่อมสภาพของตัวเร่งปฏิกิริยาผ่านการชินเทอริงของแพลทินัม การหลุดออกของโลหะ และการเกิดโค้ก การศึกษานี้อธิบายได้ด้วยวิธีการที่แข็งแกร่งขึ้นระหว่างแพลทินัมและอะลูมินา หลังจากเติม รีเนียม โรเดียม และซิลิโคทังสติก นอกจากนี้ โลหะที่สามสามารถต้านทานการเกิดโค้กบนโลหะแพลทินัมได้โดยการเคลื่อนที่ของโค้กจาก แพลทินัมไปบนตัวรองรับอะลูมินา

สาขาวิชา วิศวกรรมเคมี

ปีการศึกษา 2563

ลายมือชื่อนิสิต

ลายมือชื่อ อ.ที่ปรึกษาหลัก

ลายมือชื่อ อ.ที่ปรึกษาร่วม

6270125721 : MAJOR CHEMICAL ENGINEERING

KEYWORD: glycerin, 1,3-propanediol, 1,2-propanediol, hydrogenolysis, platinum
Therasak Tapanya : EFFECT OF THIRD METAL ON THE PERFORMANCE OF
Pt/WO_x/Al₂O₃ FOR HYDROGENOLYSIS OF GLYCEROL. Advisor: Prof. PIYASAN
PRASERTHDAM, Dr.Ing. Co-advisor: Dr. SUPAREAK PRASERTHDAM, Ph.D.

Hydrogenolysis reaction is employed to convert glycerol to valuable chemicals, especially 1,3-Propanediol. In this study, the performance, including activity, selectivity, and stability, are investigated for the third metal promoted Pt/WO_x/Al₂O₃ catalyst. The catalysts were prepared using the wet and wetness impregnation method for Pt/WO_x/Al₂O₃ and M/Pt/WO_x/Al₂O₃, respectively. The morphological properties of catalysts were examined characterized by SEM-EDX, BET, CO-chemisorption techniques. The catalytic stability was tested as a second-round hydrogenolysis reaction that the deactivation is determined by BET, CO-chemisorption, XRD, ICP, and TGA analysis. The results indicated that the addition of the third metal on Pt/WO_x/Al₂O₃ catalyst improves activity while the Re, Rh, and HSiW doped show better stability in term glycerol conversion. Nevertheless, the Re, Rh, and HSiW can improve the catalyst deactivation through Pt sintering, Pt leaching, and coking. The improvement is explained by stronger interaction between Pt and Al₂O₃ after the Re, Rh, and HSiW were added. Additionally, the third metal can against the coke formation on Pt metal as a favoured site by the moveability coke to Al₂O₃ support.

Field of Study: Chemical Engineering

Academic Year: 2020

Student's Signature

Advisor's Signature

Co-advisor's Signature

ACKNOWLEDGEMENTS

I would like to express my sincere thanks to my thesis advisor, Professor Dr. Piyasan Prasertthdam and Dr. Supareak Prasertthdam my co-advisor to give advice, guidance, suggestion, and supported during experimentation and discussion to achieve my thesis. . I am most grateful for their teaching and advice, not only the research methodologies but also many other methodologies in life. In addition, I will also be grateful to Asst. Prof. Dr. Amornchai Arpornwichanop represented as the leader. Including, Asst. Prof. Dr. Suphot Phatanasri and Assoc. Prof. Dr. Okorn Mekasuwandumrong acted as the thesis committee for a good suggestion. I would like to thank members and scientists in Center of Excellence on Catalysis and Catalytic Reaction, Faculty of Engineering, Chulalongkorn University who guide for equipment and preparation. I gratefully thank the Government Budget for financial support from NRCT-JSPS. This research is funded by Chulalongkorn University. Finally, I most gratefully acknowledge my parents and my friends; especially, Dr. Tinnakorn Saelee for all their support throughout the period of this research.



Therasak Tapanya

TABLE OF CONTENTS

	Page
.....	iii
ABSTRACT (THAI).....	iii
.....	iv
ABSTRACT (ENGLISH).....	iv
ACKNOWLEDGEMENTS	v
TABLE OF CONTENTS.....	vi
LIST OF TABLES.....	ix
LIST OF FIGURES	x
CHAPTER I.....	1
INTRODUCTION.....	1
1.1 Introduction.....	1
1.2 Objective.....	3
1.3 The Scopes of Research.....	4
1.4 Research methodology.....	5
CHAPTER II.....	6
BACKGROUND AND LITERATURE REVIEWS	6
2.1 Background of glycerol	6
2.2 Glycerol hydrogenolysis reaction to 1,3-propanediol	8
2.3 Deactivation of the heterogeneous catalyst	11
2.3.2. Metal active site sintering	12
2.3.3. Loss of active species by leaching.....	13

2.3.4. Poisoning.....	13
2.5 Literature reviews.....	14
CHAPTER III.....	19
EXPERIMENTAL	19
3.1 Chemicals.....	19
3.2 Catalyst preparation	20
3.2.1 The preparation of Pt/WO _x /γ-Al ₂ O ₃ catalyst by wet impregnation method	20
3.2.2 The preparation of M/Pt/WO _x /γ-Al ₂ O ₃ catalyst by incipient wetness impregnation method.....	21
3.3 Hydrogenolysis reaction.....	22
3.4.1 N ₂ -physisorption	24
3.4.2 Scan electron microscope (SEM).....	24
3.4.3 X-ray diffraction (XRD).....	24
3.4.4 NH ₃ -temperature programmed desorption	24
3.4.5 X-ray photoelectron spectroscopy (XPS).....	25
3.4.6 CO-pulse chemisorption.....	25
3.4.7 Thermogravimetric analysis (TGA)	25
3.4.8 Inductively coupled plasma (ICP).....	26
CHAPTER IV	27
RESULTS AND DISCUSSION.....	27
4.1 Physical Appearance.....	27
4.2 Morphological properties of the catalyst.....	27

4.3 Effect of the third metal on Pt/WO _x /γ-Al ₂ O ₃ catalyst under hydrogenolysis of glycerol	33
4.3 Effect of the third metal on catalytic stability	35
4.4 Effect of the third metal on Pt/WO _x /γ-Al ₂ O ₃ catalyst for deactivation of the catalyst.....	36
4.4.1 Effect of the third metal on metal sintering	38
4.4.2 Effect of the third metal on metal leaching	42
4.4.3 Effect of the third metal on metal-support interaction	45
4.4.3 Effect of the third metal dope on coke formation	48
CHAPTER V	51
CONCLUSION	51
5.1 Conclusion	51
5.2 Recommendations	52
5.2.1 Py-IR of catalysts should be studied to explain the selective hydrogenolysis to the wanted product	52
5.2.2 The physical surface area after Nb-doped, should be studied.....	52
APPENDIX.....	53
REFERENCES	63
VITA.....	68

LIST OF TABLES

	Page
Table 1 The Pt-WO _x based catalyst for selective hydrogenolysis of glycerol.....	15
Table 2 The precursor for the experiment.....	19
Table 3 Precursors doping on Pt/WO _x /γ-Al ₂ O ₃ catalyst.....	21
Table 4 The conditions for products analysis by using gas chromatography.....	23
Table 5 SEM image and EDX mapping of Pt/WO _x /γ-Al ₂ O ₃ catalyst and M/ Pt/WO _x /γ-Al ₂ O ₃ catalyst.....	28
Table 6 The composition elements of Pt/WO _x /γ-Al ₂ O ₃ catalyst and M/ Pt/WO _x /γ-Al ₂ O ₃ catalyst analyzed by SEM equipped EDX mode.....	29
Table 7 The N ₂ -Physisorption of Pt/WO _x /γ-Al ₂ O ₃ catalyst and M/Pt/WO _x /γ-Al ₂ O ₃ catalyst using BET analysis.....	32
Table 8 The activity of Fresh of Pt/WO _x /γ-Al ₂ O ₃ catalyst and M/ Pt/WO _x /γ-Al ₂ O ₃ catalyst in glycerol hydrogenolysis reaction under reaction conditions: 140°C and 20 bar of initial hydrogen pressure for 6 hours of reaction time.....	34
Table 9 Surface properties of fresh and used catalysts on deactivation of the catalyst.....	37
Table 10 The Pt metal crystallite size for fresh and used catalyst and the sintering of Pt metal crystallite size after hydrogenolysis reaction.....	40
Table 11 Metal leaching from surface of catalyst to aqueous phase reaction (Leaching of Pt and W) using ICP-EOS analysis.....	42
Table 12 Total coke formation and type of coke of Pt/WO _x /γ-Al ₂ O ₃ and M/Pt/WO _x /γ-Al ₂ O ₃ catalyst using TGA analysis.....	50

LIST OF FIGURES

	Page
Figure 1 Global energy consumption source [1].....	1
Figure 2 Transesterification reaction of biodiesel production [9].....	2
Figure 3 Biodiesel production via Transesterification Process adapted from [13].....	7
Figure 4 The reactions of glycerol transformation to high-value chemicals [16].....	8
Figure 5 The pathways reactions of glycerol hydrogenolysis [17]	9
Figure 6 Infographic schematic to produce Sorona® 3GT polymer	10
Figure 7 Mechanism glycerol hydrogenolysis reaction [24].....	11
Figure 8 Conceptual model of coke formation [26]	12
Figure 9 Mechanisms for crystallite growth as sintering [26].....	12
Figure 10 A model of a supported metal particle, illustrating the effects of metal-support interfacial interactions	14
Figure 11 Schematic of Pt/WO _x /γ-Al ₂ O ₃ catalyst preparation by wet impregnation method.....	20
Figure 12 Schematic of preparation for the catalyst M/Pt/WO _x /γ-Al ₂ O ₃ by incipient wetness impregnation method.....	21
Figure 13 An autoclave reactor system	22
Figure 14 Physical Appearance of fresh catalyst (a) Pt/WO _x /γ-Al ₂ O ₃ (b) Re/Pt/WO _x /γ-Al ₂ O ₃ (c) Rh/Pt/WO _x /γ-Al ₂ O ₃ (d) Nb/Pt/WO _x /γ-Al ₂ O ₃ and (e) HSiW/Pt/WO _x /γ-Al ₂ O ₃	27
Figure 15 Catalytic stability in terms of fresh catalyst comparing used catalyst under hydrogenolysis reaction.....	36
Figure 16 XRD patterns of fresh and used Pt/WO _x /γ-Al ₂ O ₃ and M/Pt/WO _x /γ-Al ₂ O ₃ catalyst (M represent Re, Rh, Nb, and HSiW).....	39

Figure 17 The semi-log graph between Pt sintering (%) and difference of electronegativity value (ΔEN).....	41
Figure 18 The correlation between Pt leaching (%) and difference of electronegativity value (ΔEN).....	43
Figure 19 The correlation between W leaching (%) and difference of electronegativity value (ΔEN)	44
Figure 20 Schematic of Metal-Support interaction	45
Figure 21 XPS spectra of Pt-4f for (a). Pt/WO _x /Al ₂ O ₃ and (b). Re/Pt/WO _x /Al ₂ O ₃ (c). Rh/Pt/WO _x /Al ₂ O ₃ (d). Nb/Pt/WO _x /Al ₂ O ₃ (e). HSiW/Pt/WO _x /Al ₂ O ₃ . Note that the red, blue, and green peaks are represented to Pt ⁰ , Pt ²⁺ , and Pt ⁴⁺ respectively	47
Figure 22 TPO analysis for (a). Pt/WO _x /Al ₂ O ₃ and (b). Re/Pt/WO _x /Al ₂ O ₃ (c). Rh/Pt/WO _x /Al ₂ O ₃ (d). Nb/Pt/WO _x /Al ₂ O ₃ (e). HSiW/Pt/WO _x /Al ₂ O ₃	49

CHAPTER I

INTRODUCTION

1.1 Introduction

Nowadays, energy consumption is indispensable for the economy and social advancement of all societies in the world. Certainly, resource availability of energy is necessary to sufficiently utilize due to the impossibility of suppressing the rate of global population growth. Since the 19th century, fossil fuels, like crude oil, coal, and natural gas, are the fundamental global primary energy source, that there is a trend of increasing demand continuously (see Figure 1) [1]. Industrial manufacturing has primarily employed it for transportation fuels, chemical products, utility systems, etc.[2].

Although the comfortable human life from these utilities, the combustion of fossil fuels was effective for greenhouse gas emissions, especially carbon dioxide, leading to a rise in the average climate temperature of the earth, which contributes to global warming [3].

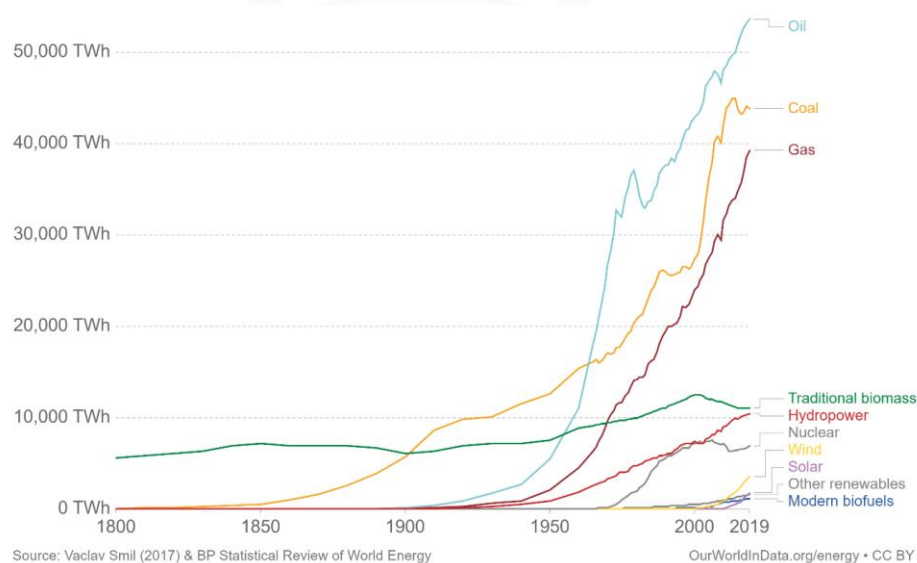


Figure 1 Global energy consumption source [1]

As a consequence of the issue related to increased carbon dioxide emission, a renewable resource, sustainable alternatives have extremely attracted to produce bioenergy and chemical products due to green process. Less carbon dioxide emission and its enhanced use would address several societal needs.[4]. Among the developments for the issue, biodiesel is a renewable energy that has become more graceful recently since it prevented a further increase of carbon dioxide emissions in practical [5, 6].

Typically, biodiesel production has been converted from biomass-derived such as palm oil, coconut, soybean, etc., via transesterification with alcohol to form methyl ester- biodiesel, which produces glycerol as a by-product as shown in Figure 2 [7]. Generally, biodiesel production comprises 10%(w/w) glycerol (10 tons of biodiesel with one ton of glycerol). Consequently, the rapid expansion of biodiesel production worldwide brings a redundant amount of glycerol into the market due to low value and demand [8].

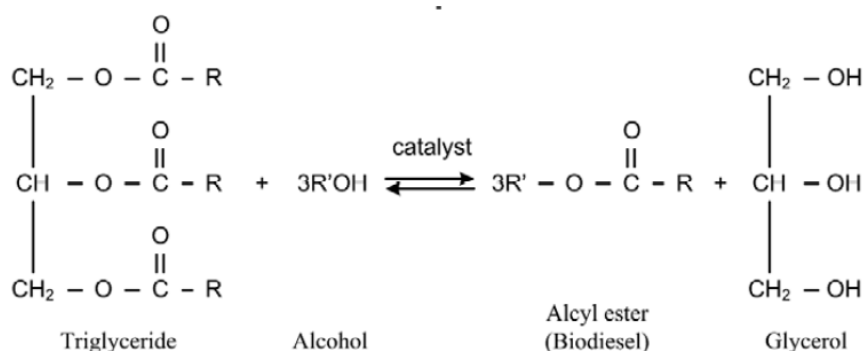


Figure 2 Transesterification reaction of biodiesel production [9]

Even though the market of glycerol is small, the structure of glycerol contains three hydroxyl groups, which can transform into valuable chemicals [9]. To reduce the manufacturing of biodiesel production for a decreased amount of glycerol is

impossible due to society's high demand energy consumption; hence finding a new way to convert glycerol to high-value chemicals, especially the hydrogenolysis of glycerol to 1,3-propanediol is very interested because it is used for much application such as produced polytrimethylene terephthalate (PTT) and used as a chemical intermediate for polyether, polyurethanes, and polyesters production.

However, the hydrogenolysis reaction can be achieved by requiring hydrogen activation. Therefore, metal catalysts, especially noble metal catalysts, have been selected. Up to now, the Pt/WO_x based catalyst has been widely employed since the synergies of Pt metal sites, and WO_x as an acid site provides the mechanism of hydrogenolysis reaction to increasing selectivity of 1,3-propanediol [10].

Undoubtedly, the deactivation of catalysts is the fundamental factor that occurs during the reaction for the industry's catalytic process especially the liquid phase hydrothermal reaction because the life of the catalyst directly affects the production cost of the product. To modify the stability of catalysts, the promoter's role in improving the catalyst stability by metal doping is another route to prevent deactivation that has been reported [11].

Herein, the modification of Pt/WO_x/γ-Al₂O₃ catalyst by metals doping as a promoter is investigated during the hydrogenolysis reaction. Understanding the catalyst's deactivation, the roles of promoters on prevention deactivation of Pt/WO_x/Al₂O₃ catalyst are also focused.

1.2 Objective

To study the roles of the third metals as a promoter on Pt/WO_x/γ-Al₂O₃ catalyst for the performance of glycerol hydrogenolysis to 1,3-Propanediol under mild reaction conditions

1.3 The Scopes of Research

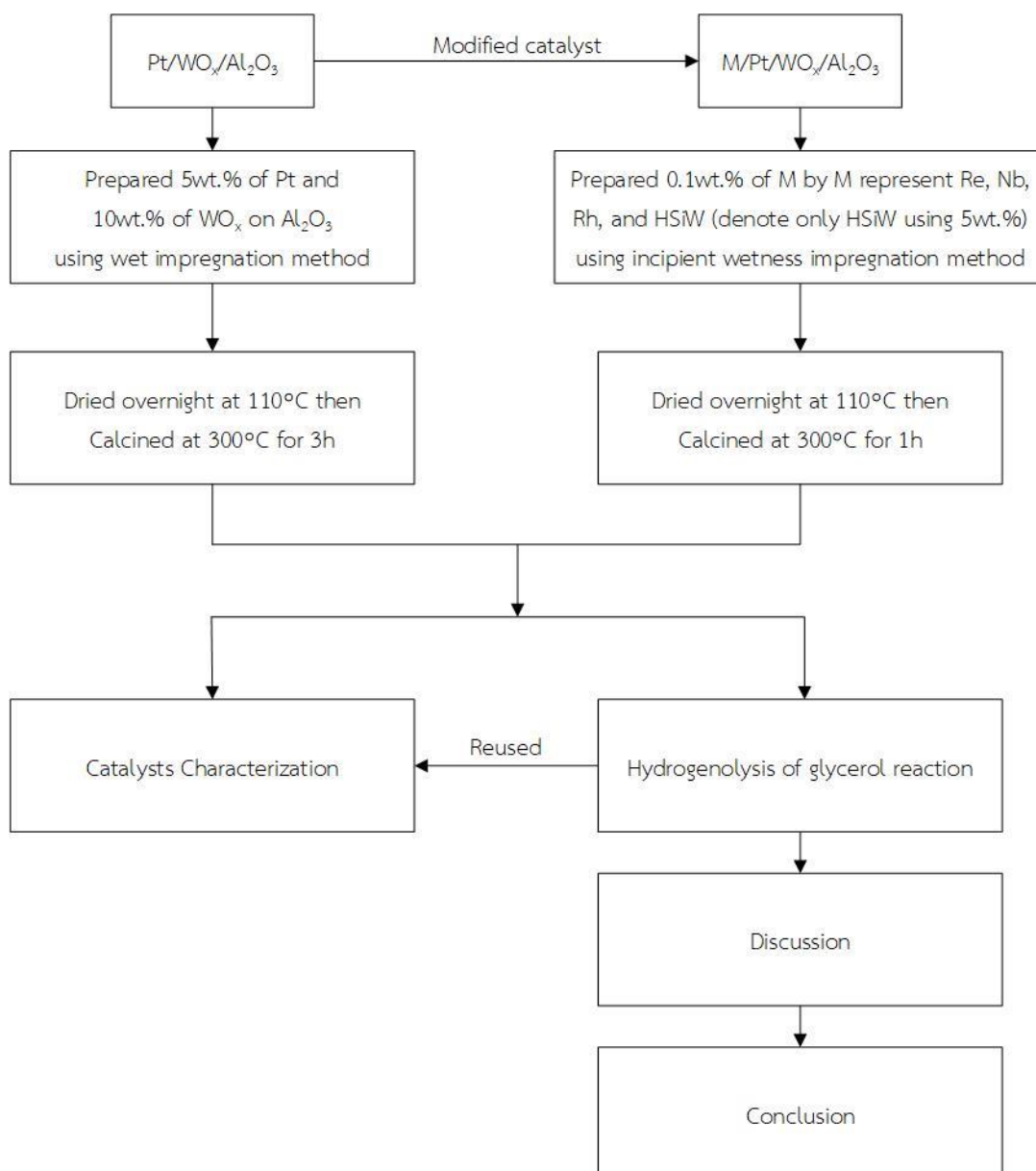
1.3.1 Studying the catalytic activity for Pt/WO_x/γ-Al₂O₃ and M/Pt/WO_x/γ-Al₂O₃ (M are the third metals consist of Rh, Re, Nb, and HSiW) via hydrogenolysis of glycerol under conditions 20 bar of initial hydrogen pressure and 140°C of system temperature for 6 hours

1.3.2 Studying catalytic stability in terms of fresh and used catalyst for hydrogenolysis reaction

1.3.3 Studying the promoter roles for retarding catalytic deactivation of modified Pt/WO_x/γ-Al₂O₃ catalyst during hydrogenolysis reaction (leaching, sintering, and coke formation)



1.4 Research methodology



CHAPTER II

BACKGROUND AND LITERATURE REVIEWS

In the previous chapter, the excessive quantity of glycerol leads to a less valuable economic market was mentioned. Therefore, the added value of glycerol to other chemicals by hydrogenolysis reaction has been attentive in this thesis. The backgrounds and the general information about glycerol hydrogenolysis are mentioned in this section. The catalytic activity of glycerol conversion corresponding with yield of wanted 1,2-PDO and 1,3-PDO production as well as catalytic deactivation is also clarified in this section.

2.1 Background of glycerol

Glycerol, also called glycerine, is the polyol compound obtained as the main by-product out of biodiesel production via transesterification of vegetable oils or animal fats (Figure 3). In the past, glycerol was synthesized from propylene involving the use of O_2 or Cl_2 production. However, the great deal of glycerol obtained as a by-product of biodiesel production has affected the production of glycerol from other resources resulted to decrease in glycerol production from another process. Moreover, rapidly increased glycerol production from biodiesel production leads to consumption of crude glycerol in the market is a serious issue of financial and environmental liability due to abundant glycerol [12]. Recently, Dow Chemical and Solvay companies have recirculated the glycerol epichlorohydrin production for profitability and inhibited the increase of glycerol obtained biodiesel conversion process [13]. Moreover, increased glycerol from the biodiesel process has converted to valuable chemicals via several processes for example cyclization, dehydration, esterification, etherification, oligomerization, reforming, and hydrogenolysis reaction.

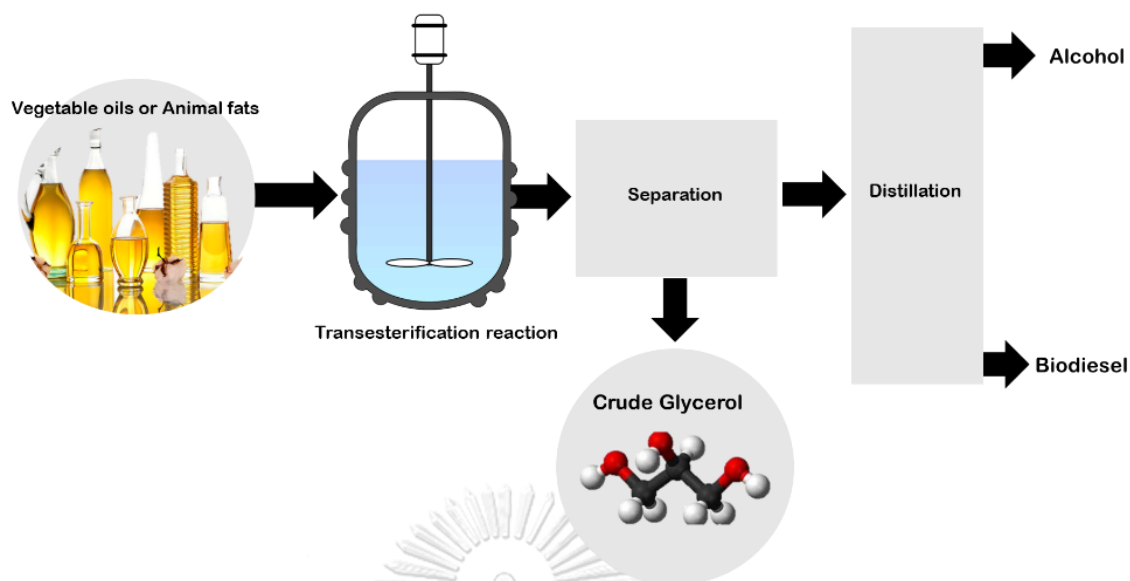


Figure 3 Biodiesel production via Transesterification Process adapted from [13]

Commonly, the traditional glycerol can be applied as a precursor for manufacturing cosmetics, foods, alkyl resins, pharmaceuticals, polyurethane, etc. [14]. However, crude glycerol from the biodiesel process has contaminants such as alcohol, catalyst, and unreacted fatty acid, which is a crucial issue and low value; therefore, the distillation process for removing impurities is needed. Accordingly, transforming glycerol into high value-added chemicals has been dramatically attracted which all possibilities of glycerol conversion are shown in figure 4. Among the various reactions, the hydrogenolysis reaction to polyols such as 1,2-propanediol and 1,3-propanediol has more focus due to the high C/O ratio of glycerol structure which appropriates for hydrogenolysis reaction [15, 16].

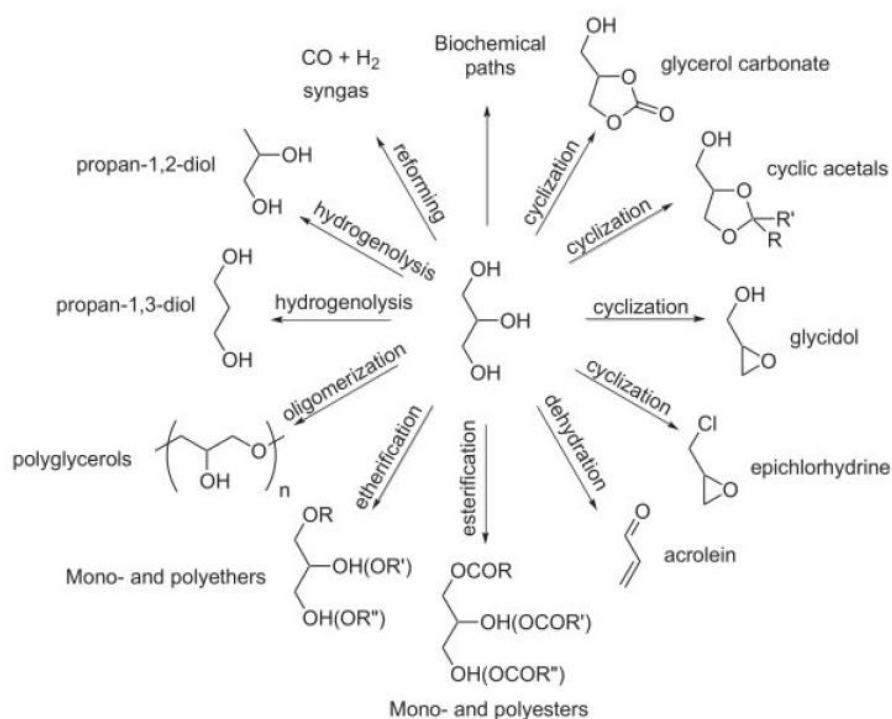


Figure 4 The reactions of glycerol transformation to high-value chemicals [16]

2.2 Glycerol hydrogenolysis reaction to 1,3-propanediol

Hydrogenolysis reaction is a chemical reaction that can be undergone by hydrogenated the single bond of C-C or C-heteroatom which the heteroatom refers to oxygen, nitrogen, or sulfur [17]. Due to the glycerol structure contains three-carbon atoms with three hydroxyl groups providing a high C/O ratio that the hydrogenolysis reaction results in the glycerol conversion to useful chemical products [16]. Additionally, the hydrogenolysis of glycerol is the competitive reaction between C-O cleavage of the primary and secondary hydroxyl groups generating the different forms of 1,2-propanediol and 1,3-propanediol, respectively. Moreover, other side products of 1-propanol, 2-propanol, and propane are also possible to taken place. Moreover, the C-C bond of glycerol can be cleaved to form ethylene glycol, ethanol, methanol, and methane as illustrated in figure 5 [16, 18].

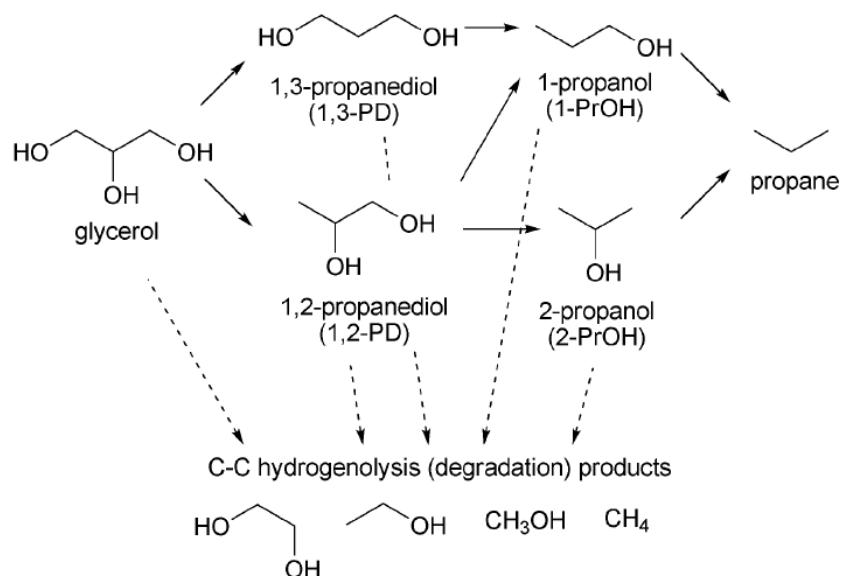


Figure 5 The pathways reactions of glycerol hydrogenolysis [17]

Among the various products, the commercial interest of 1,3-propanediol has extrapolated for the long profitability on a large scale in the industry as diverse applications, for instance, monomer, rug fibers and textile, cosmetics, paint manufacturing, and cleaning products, etc. [19]. Specifically, to produce polytrimethylene terephthalate (PTT) as a polymer platform for the future, employed in resins and fibers manufacturing that introduce 90% of 1,3-propanediol in the component. Presently, PTT is a valuable polymer that leads to producing 0.1 million tonnes per year in the market [20]. Moreover, there are applications of 1,3-propanediol in commercial-grade especially, the 1,3-propanediol has developed under brands Susterra® and Zemea® propanediol to produce Sorona® 3GT polymer from fermentation by DuPont Tate & Lyle Bio Products that use for the textile industry as shown in figure 6 [21].

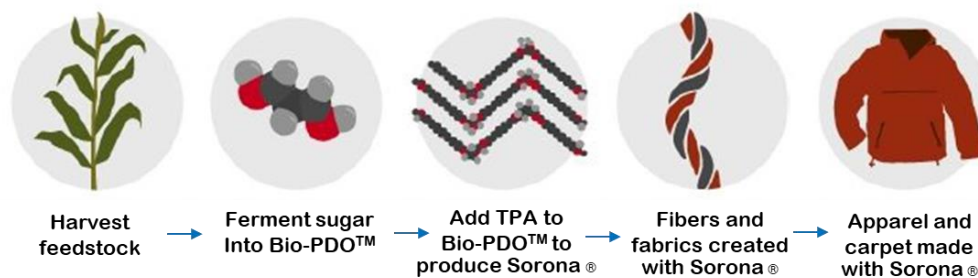


Figure 6 Infographic schematic to produce Sorona® 3GT polymer

However, the fermentation process has limitations about the complicated process such as high sensitivity to change the system and difficult separation of the enzyme from products, etc. [22]. Hence, hydrogenolysis is a candidate reaction for convert glycerol to 1,3-propanediol with the heterogeneous catalyst for the promising process to developed to commercial-grade.

Generally, the hydrogenolysis reaction involves combining a two-step reaction: dehydration and hydrogenation, as shown in figure 7. For the first step, glycerol is dehydrated under acidic catalyst via dehydration reaction producing hydroxy acetone (HA) and 3-hydroxy propionaldehyde (3-HPA). Then, hydroxy acetone (HA) and 3-hydroxy propionaldehyde (3-HPA) can be hydrogenated on the metal catalyst to form 1,2-propanediol and 1,3-propanediol. Due to the thermodynamically easy formation of acetal than 3-hydroxy propionaldehyde, it's difficult to obtain 1,3-propanediol. Therefore, increasing the yield of 1,3-propanediol is a challenge which catalyst approaches are ascribed in the literature review [23].

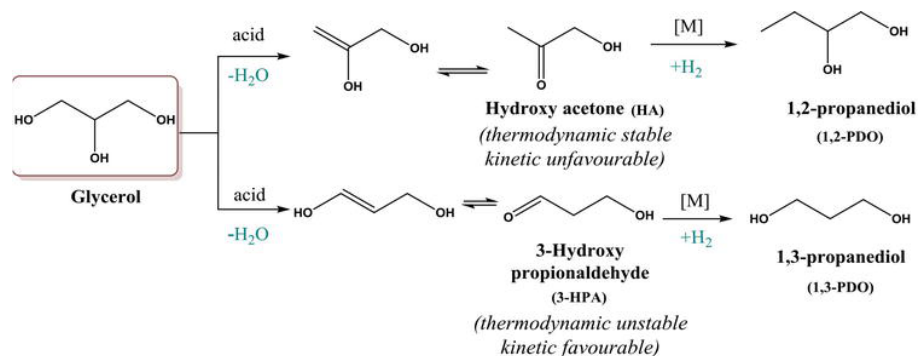


Figure 7 Mechanism glycerol hydrogenolysis reaction [24]

2.3 Deactivation of the heterogeneous catalyst

Nowadays, deactivation has been realized for aspects of the industrial catalytic processes because the effect of stability and reusability of the catalyst is another factor that reduces the operating cost of the process. Generally, the deactivation leads to the deactivation of the catalytic activity of the used catalyst. The deactivation of the catalyst consists of carbon deposition or fouling, metal active site sintering, loss of active species by leaching, and poisoning. For detail of each factor are particularized in the next section.

2.3.1. Carbon deposition or fouling

Fouling, the type of chemicals from the fluid phase, mechanically deposits onto the catalyst surface, leads to blocking the active sites of catalyst (Figure 8). Besides, fouling by carbon deposit is called coking that is formed during the reaction. Usually, the coke formation can be generated from several causes especially, the high-temperature conditions. Coke formation is initiated by atomic carbon adsorption on the surface of the catalyst. After that, coke deposition to form graphitic is formed that hard to oxidize [11]. Additionally, the acidity of catalyst appropriate for hydrogenolysis reaction is another effect of the coke formation. Therefore, the deactivation of catalysts by coking in this process should also be emphasized [24].

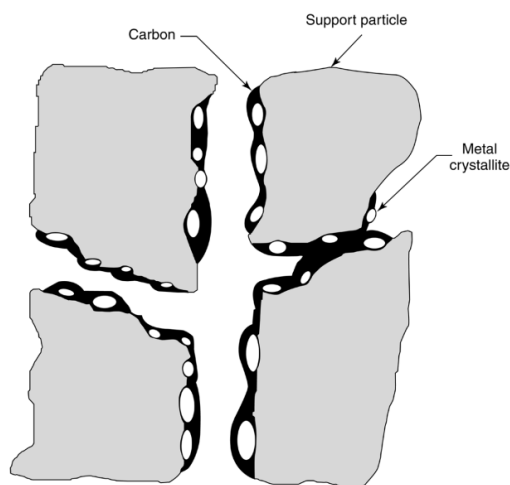


Figure 8 Conceptual model of coke formation [26]

(Copyright 2006, Wiley-Interscience)

2.3.2. Metal active site sintering

One of the catalyst deactivations under high-temperature reaction is the sintering that affects the loss of active metal surface by accumulation of metal site to form inactive metal species. Usually, sintering can be taken place in high-temperature reactions. Moreover, present of water vapor in the system accelerates the sintering. Additionally, crystallite growth caused by sintering has fundamental mechanisms—crystallite migration, atomic migration, and vapor transport (Figure 9) [24].

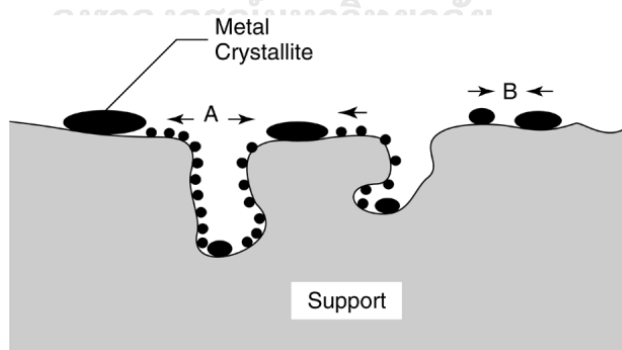


Figure 9 Mechanisms for crystallite growth as sintering [26]

(Copyright 2006, Wiley-Interscience)

2.3.3. Loss of active species by leaching

For the liquid phase reaction, the loss of active species by leaching contributes to the main cause of the catalyst deactivation. In the leaching process, the catalyst is extracted to fall-off by liquid phase preferably, for loss of active site on the support; as a result, to declining of catalyst performance with can be taken please under liquid phase condition [25].

2.3.4. Poisoning

The deactivation by poisoning can occur by of the strong chemisorption on active sites and intermediate that lead to poaching the sites for reaction. Generally, the chemicals which adsorb are reactants, products, or impurities; they are temporary or permanent that are as a result reversible or irreversible, respectively. Normally, poisoning is permanent on the sites that irreversible since the loss of active sites for the reaction [24].

2.4 Metal-Support interaction

Metal nanoparticles are stabilized on the support material catalyst that is the factor key of reaction for the catalytic process because it affects the state of metal on the support material which can explain the chemical reaction and the interaction between the metal and support. Additionally, the metal-support interaction can be used to explain the deactivation from leaching and sintering metal because the strong interaction of metal on the support can reduce the agglomeration and leaching by solvation. Understanding the metal-support interaction, the effect of electronic properties was considered to show the stronger and weaker metal-support interaction. In 1992, Jose and coworkers investigate the properties, electronegativity value, of the electronic change of metal and metal on the bimetallic surface, resulted in the bonding of metal and metal and metal and support. Moreover, they show the high electronegativity value of metal influent the alloy formation [26]. Additionally, Chun-Jern Pan and coworkers explain the strong metal-support interaction (SMSI) in heterogeneous catalysis that figure 10 shows A model of a supported metal particle, illustrating the effects of metal-support interfacial interactions. Form this study, the explained the metal-support interaction (SMSI) in heterogeneous catalysis can occur by electrons from support is transferred to the

metal on the support material brought the stronger interaction on the support material.

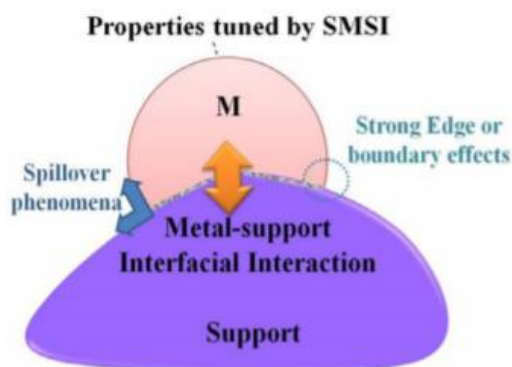


Figure 10 A model of a supported metal particle, illustrating the effects of metal-support interfacial interactions

2.5 Literature reviews

From previous, mention about the background detail which brings information to describe appropriate catalyst use for hydrogenolysis of glycerol reaction to increase 1,3-propanediol yield and to realize deactivation of the catalyst during the reaction for long live catalyst are review in the part of literature reviews.

Considering the catalyst have used to increase 1,3-propanediol yield focuses on activation of the secondary hydroxyl cleavage during hydrogenolysis process. Typically, the conventional catalysts including noble metals and transition metals are used for hydrogenolysis of glycerol such as Pt, Ru, Pd, Cu, and Ni because they provide the high catalytic activity to activate hydrogen molecules [27, 28]. The feature of the non-noble metal or transition metal catalyst have been considered because of the low price, which is the advantage for improving the operating cost of the process in the future. Although the non-noble metal catalyst has been attended, the problems of easily coke formation in liquid reaction and selectivity of 1,2-propanediol production as the main product limits using non-noble catalyst for hydrogenolysis of glycerol [9, 29]. To overcome the problems, noble metal has been

widely employed although its cost is very high. Hence, improvement of catalytic stability should be gained an attention for using noble metal catalyst.

Among these precious metal catalysts for hydrogenolysis of glycerol reaction, The bimetallic platinum-tungsten oxide-based catalyst provides an attractive properties in terms of high selectivity of 1,3-propanediol production and high reactivity of glycerol conversion, as concluded in table 1.

Table 1 The Pt-WO_x based catalyst for selective hydrogenolysis of glycerol

Entry	Catalyst	Temperature (°C)	Pressure (bar)	Time (h)	Conversion (%)	1,3-PDO Selectivity (%)	Ref.
1	Pt/WO _x	160	10	12	16.1	34.0	[30]
2	Pt/m-WO _x	180	55	12	18.0	39.3	[31]
3	Pt/WO _x /ALOOH	180	50	12	100	66.0	[32]
4	Pt-ALO _x /WO ₃	180	30	10	90.0	44.4	[33]
5	Pt/WO _x /γ-Al ₂ O ₃	200	45	24	53.1	51.9	[34]

Jia Wang and coworkers synthesized Pt on mesoporous WO_x, which provides high dispersion of Pt. The outstanding of this work show the activity for hydrogenolysis of glycerol to 1,3-propanediol at 160°C and 10 bar hydrogen pressure for 12 h with high space-time velocity yield 3.78 g•g_{Pt}⁻¹h⁻¹. The catalyst characterization results show that abundant oxygen vacancies of WO_x lead to increased dispersion of Pt as a single/pseudo-single atom, which excellently dissociates H₂ at the interface of WO_x and can provide brønsted acid sites toward increase 1,3-propanediol selectivity [30].

Additionally, LIU Longjie's group has compared the commercial WO₃ (c-WO₃) and mesoporous WO₃ (m-WO₃) that was synthesized using an evaporation-induced self-assembly method; these are the support of Pt for hydrogenolysis of glycerol. In comparison, the performance of Pt/m-WO₃ more active than Pt/c-WO₃, which shows

high dispersion of Pt and easily reducible WO_3 that facilitates the heterolytic dissociation of H_2 [31].

Although Pt- WO_x catalyst shows the better result for increasing 1,3-propanediol selectivity, the activity of glycerol conversion is still required. However, acidic supports with high surface area properties such as zirconia, silica, titania, and alumina have been used to modify Pt/ WO_x catalyst. These promote well dispersion of WO_x to form WO_x species, which can generate strong Brønsted acidity that improves conversion and selectivity of 1,3-propanediol.[35-38].

Interestingly, Racha Arundhathi and coworkers investigated the hydrogenolysis of glycerol to 1,3-propanediol under 180°C and 50 bar of hydrogen pressure using AlOOH as support. The result shows the performance of Pt/ WO_x / AlOOH catalyst complete reaction for 12 h with 66% selectivity of 1,3-propanediol [32]. In a previous work reported by the same group, they study the addition of AlO_x for glycerol hydrogenolysis to selective 1,3-propanediol, which also obtain the high selectivity of 1,3-propanediol (44.4%) [33].

Consequently, results obtained, they proposed that the increasing 1,3-propanediol by adsorbing the glycerol on the Al-OH group and generate Al-alkoxide species then the Pt atoms are activated H_2 to H atoms and spill over to Al-alkoxide. Finally, The Al-alkoxide reacts with H atoms via hydrogenation reaction to formation 1,3-propanediol. However, this hypothesis is still controversial to explain the mechanism because the formation of Al-alkoxide is not proved. Moreover, the XRD result shows that the presence of difference alumina structures possibly $\gamma\text{-Al}_2\text{O}_3$ under the high temperature uses for pretreatment leads to the absence of the hydroxyl group.

According to developing Pt/ WO_x / AlOOH carried out by Racha Arundhathi and coworkers, The Pt/ WO_x / $\gamma\text{-Al}_2\text{O}_3$ catalyst has attracted to hydrogenolysis of glycerol to 1,3-propanediol. In 2015, García-Fernández and coworkers studied the hydrogenolysis of glycerol to 1,3-propanediol using Pt/ WO_x / $\gamma\text{-Al}_2\text{O}_3$ catalyst. They investigate the effect of Pt and WO_x amount on glycerol conversion and 1,3-propanediol selectivity. The results illustrate the Pt are the main active sites for convert glycerol to formation

products. Furthermore, the 1,3-propanediol selectivity depends on the surface density of the tungsten, which plays an important role in the acidity of the catalyst to produce 1,3-propanediol. Moreover, the results indicate that the Pt content not only affects the glycerol conversion but also has interaction with WO_x content, which promotes the formation of 1,3-propanediol formation [34].

Although the $Pt/WO_x/\gamma-Al_2O_3$ catalyst is widely used and has shown more significant potential for hydrogenolysis of glycerol to 1,3-propanediol, the catalyst stability still pays little attention from researchers. In 2020, Nian Lei et al. studied the stability of the $Pt/WO_x/\gamma-Al_2O_3$ catalyst in the glycerol hydrogenolysis of 180°C and the 50 bar of hydrogen pressure. The studies have shown that over 700 hours of reaction, the stability of the catalyst has decreased. And from the analysis of the catalyst characterization of the catalyst after the glycerol hydrogenolysis reaction, it was found that the size of Pt metal became larger due to the leaching of tungsten metal during the reaction. The Pt metal growth has resulted from the Pt agglomeration, causing the Pt metal to become larger [39].

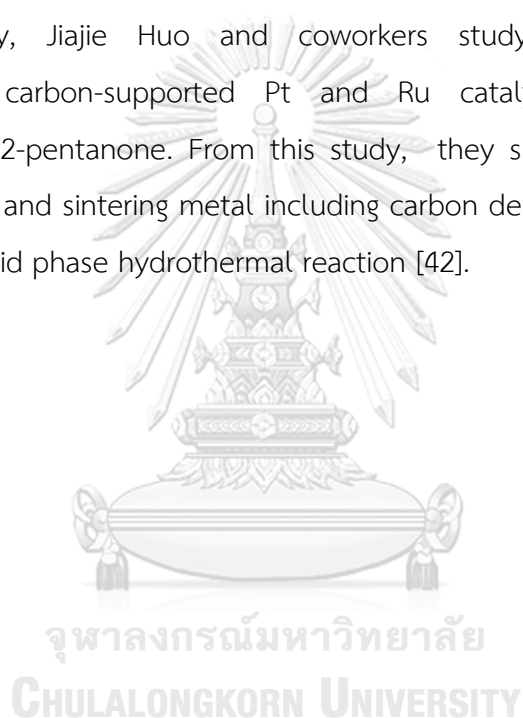
Recently, Tinnakorn Saelee and coworkers studied the roles of WO_x in the $Pt/\gamma-Al_2O_3$ catalyst. The comparison of $Pt/\gamma-Al_2O_3$ and $Pt/WO_x/\gamma-Al_2O_3$ catalysts on the catalytic activity of glycerol conversion and selectivity of 1,3PDO production were investigated. They found that the performance of used catalysts is decreased due to the leaching of Pt on the surface catalyst, especially $Pt/\gamma-Al_2O_3$ catalyst. Furthermore, the presence of WO_x plays an important role in terms of increment of Pt- Al_2O_3 interaction preventing the Pt agglomeration. Moreover, existence of WO_x promotes the electron donor from Pt to $\gamma-Al_2O_3$ surface[40].

In the industry, the stability of the catalyst is the most important because the long life of the catalyst leads to the catalyst reusability resulting in reduced operation cost. The development of $Pt/WO_x/\gamma-Al_2O_3$ catalyst, Jia Wang and coworkers reported the modified $Pt/WO_x/\gamma-Al_2O_3$ catalyst by doping promoters including the precious metals (such as Ru, Ir, and Rh) and transition metals (such as Re, La, Fe, Zr, Sn and Ce oxides) under glycerol hydrogenolysis reaction. They showed that some metals a promoting the increasing 1,3-propanediol. Additionally,

they illustrated the hydrogenolysis reaction for 85 hours, in which the addition promoters can improve the stability of the Pt/WO_x/γ-Al₂O₃ catalyst [41].

However, they have not mentioned the roles of promoters in the prevention deactivation. Therefore, this research is focused on the roles of promoters, including transition metals (Re and Nb), precious metal (Rh), and heteropoly acid; HPAs (HSiW: silicotungstic acid) are modified on Pt/WO_x/γ-Al₂O₃ catalyst to regarding the deactivation (Leaching, Sintering, and Coking) under the glycerol hydrogenolysis in liquid phase reaction.

Additionally, Jijie Huo and coworkers study the deactivation and regeneration of carbon-supported Pt and Ru catalysts in aqueous phase hydrogenation of 2-pentanone. From this study, they show the deactivation can occur via leaching and sintering metal including carbon deposition or coke formation process under liquid phase hydrothermal reaction [42].



CHAPTER III

EXPERIMENTAL

In this chapter, the procedure of experimental includes employed chemicals, catalysts preparation, catalytic performance test via hydrogenolysis reaction, and catalysts characterization is introduced. In detail, The conditions for the experiment are introduced. Additionally, the apparatus, schematic, and specification of instruments are concluded.

3.1 Chemicals

The precursor used as chemicals for catalyst synthesis and the glycerol hydrogenolysis reaction is detailed in table 2.

Table 2 The precursor for the experiment

Chemicals	Chemical formula	Supplier
Alumina (lab grade)	$\gamma\text{-Al}_2\text{O}_3$	Kemaus
Glycerol	$\text{C}_3\text{H}_8\text{O}_3$	Sigma-Aldrich
Chloroplatinic acid hydrate	H_2PtCl_6	Sigma-Aldrich
Ammonium(meta)tungstate hydrate	$(\text{NH}_4)_6\text{H}_2\text{W}_{12}\text{O}_{40}\cdot n\text{H}_2\text{O}$	Sigma-Aldrich
Ammonium perrhenate	NH_4ReO_4	Sigma-Aldrich
Rhodium (III) chloride	RhCl_3	Sigma-Aldrich
Niobium(V) chloride	NbCl_5	Sigma-Aldrich
Tungstosilicic acid hydrate	$\text{H}_4(\text{W}_{12}\text{SiO}_{40})$	Sigma-Aldrich

3.2 Catalyst preparation

The catalysts preparation via different methods, including the preparation of Pt/WO_x/γ-Al₂O₃ catalyst and modified Pt/WO_x/γ-Al₂O₃ by the promoter as described M/Pt/WO_x/γ-Al₂O₃ which M are represented promoters include Re, Nb, Rh, and HSiW. In the following sections, the preparation methods are mentioned.

3.2.1 The preparation of Pt/WO_x/γ-Al₂O₃ catalyst by wet impregnation method

The Pt/WO_x/γ-Al₂O₃ catalyst was synthesized by followed the schematic in Figure 11. Firstly, the Ammonium Metatungstate Hydrate (AMT, (NH₄)₆H₂W₁₂O₄₀·nH₂O, ≥99.99%) was used as a precursor for WO_x, which was impregnated on the γ-Al₂O₃ support by using 10wt.% of WO_x on γ-Al₂O₃ support. Then, the WO_x/γ-Al₂O₃ was dried at 110°C overnight. Then, the dried powder was calcined in static air at 900°C for 3 hours.

To obtain the Pt/WO_x/γ-Al₂O₃ catalyst, WO_x/γ-Al₂O₃ powder that was prepared was impregnated with 5wt.% of Pt by using chloroplatinic acid hydrate (H₂PtCl₆) as a precursor. After that, the slurry was evaporated at 110°C overnight before purifying at 300°C for 3 hours under stagnant air.

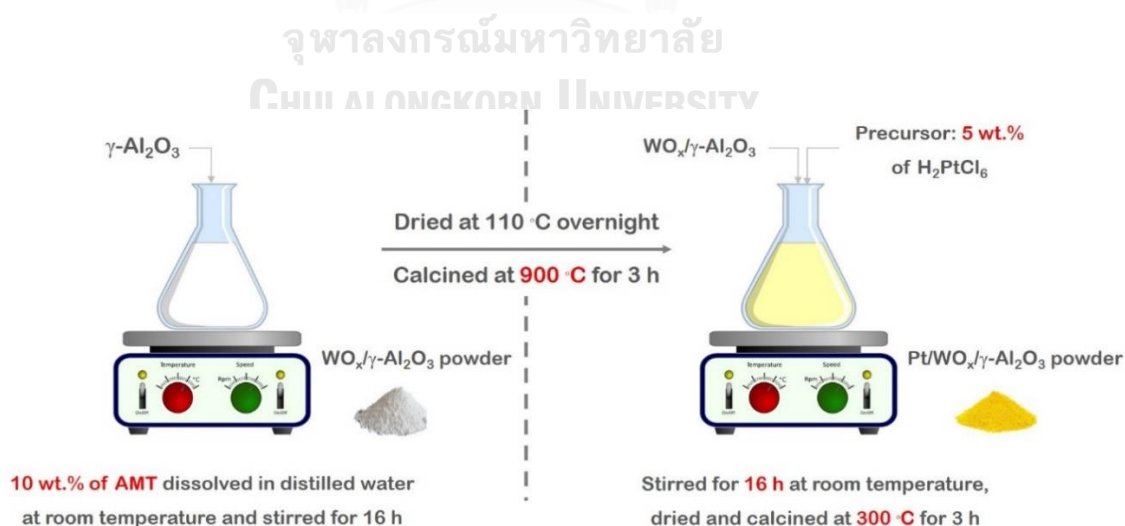


Figure 11 Schematic of Pt/WO_x/γ-Al₂O₃ catalyst preparation by wet impregnation method

3.2.2 The preparation of $M/Pt/WO_x/\gamma-Al_2O_3$ catalyst by incipient wetness impregnation method

For $M/Pt/WO_x/\gamma-Al_2O_3$ catalyst by M represent Re, Nb, Rh, and HSiW, the M metal was also impregnated into $Pt/WO_x/\gamma-Al_2O_3$ incipient wetness impregnation method by using precursors doping on $Pt/WO_x/\gamma-Al_2O_3$ catalyst as shown in table 3. And then, the wet solid was dried at $110^\circ C$ overnight and calcined at $300^\circ C$ for 1 hour. Figure 12 shown schematically of preparation for the catalyst $M/Pt/WO_x/\gamma-Al_2O_3$ by incipient wetness impregnation method.

Table 3 Precursors doping on $Pt/WO_x/\gamma-Al_2O_3$ catalyst

Precursors for metal doping (M)	Chemical formula	Wt. %
Ammonium perrhenate	NH_4ReO_4	0.1
Rhodium (III) chloride	$RhCl_3$	0.1
Niobium(V) chloride	$NbCl_5$	0.1
Tungstosilicic acid hydrate	$H_4(W_{12}SiO_{40})$	5

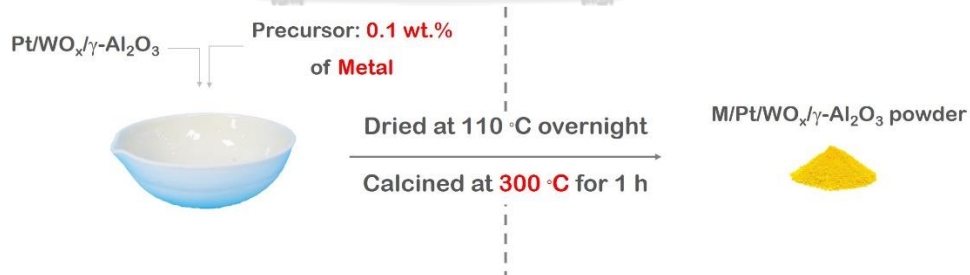


Figure 12 Schematic of preparation for the catalyst $M/Pt/WO_x/\gamma-Al_2O_3$ by incipient wetness impregnation method

3.3 Hydrogenolysis reaction

The catalytic reaction for hydrogenolysis of glycerol to 1,3-propanediol was performed under the liquid phase. The 3 wt.% glycerol aqueous solution with 0.6 g of catalyst was set into the reactor as a stainless-steel autoclave, which is shown in figure 13. Then, the system was purged and pressurized with the 20 bar of hydrogen at least three times. Then, the temperature was ramped up to the temperature reaction at 140°C by continuously stirring at 800rpm. The reaction time was set as 6 hours. When the reaction was completed, the temperature was immediately cooled down to room temperature.

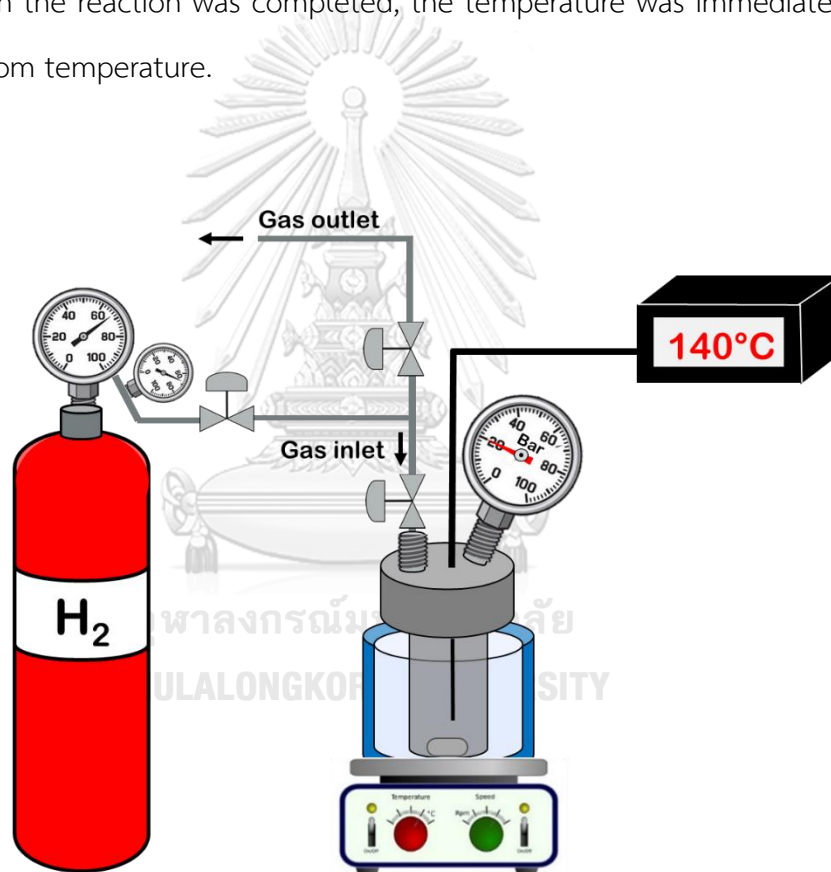


Figure 13 An autoclave reactor system

For product analysis, the obtained products using ethylene glycol as an internal standard were analyzed using a Shimadzu 14B gas chromatograph DB-WAX-UI capillary column with flame ionization detector (30m x 0.32mm x 0.5 μ m) by the

details were summarized in table 4. The glycerol conversion, selectivity, and C₃ Moles Balance were calculated using the following Eq. (1), Eq. (2), and Eq. (3), respectively.

$$\text{Glycerol conversion (\%)} = \frac{\text{moles of glycerol (in)} - \text{moles of glycerol (out)}}{\text{moles of glycerol (in)}} \times 100 \quad (1)$$

$$\text{Selectivity (\%)} = \frac{\text{moles of product}}{\text{moles of glycerol (in)} - \text{moles of glycerol (out)}} \times 100 \quad (2)$$

$$\text{C}_3 \text{ Balance (\%)} = \frac{\sum \text{mass of product} + \text{mass of glycerol (out)}}{\text{mass of glycerol (in)}} \times 100 \quad (3)$$

Table 4 The conditions for products analysis by using gas chromatography

Injector	Volume injected	0.4 μ L
	Inlet temperature	60°C
	Carrier gas	Helium (99.99 vol.%)
Column	Initial Temperature	60°C
	Hold	10 min
	Ramp ₁	10 °C/min
	Final temperature	250°C
Detector	Detector temperature	250°C
	Detector	FID
	Make-up gas	Air (99.9 vol.%)

3.4 Catalysts characterization

The various characterization techniques of catalyst were used to understand the properties of the catalyst, which include the textural and chemical properties by following procedures are detailed below.

3.4.1 N₂-physisorption

The fresh and used catalysts were analyzed to identify the surface area by N₂ physisorption using the Micromeritics Chemisorb 2750 Pulse Chemisorption system with a single point N₂ adsorption isotherm technic. For surface pretreatment of catalyst, 50mg was prepared in U-tube to equip with the heater at 300°C under N₂ flow for 1hour. After that, the system was cooled down to ambient temperature. For N₂ adsorption, the temperature was reduced to -196°C under 30%N₂/He flow. Finally, the desorption was evaluated by increasing the temperature to room temperature. The amount of adsorption and desorption N₂ was calculated for the specific surface area of the catalysts.

3.4.2 Scan electron microscope (SEM)

The morphological properties of fresh and used catalysts were characterized using scanning electron microscopy combined with energy dispersive X-ray analysis (SEM/EDX; JEOL model JSM-5800LV) to analyze the dispersion of the elements on the support.

3.4.3 X-ray diffraction (XRD)

To characterize crystallography of fresh and used catalyst, Powder X-ray diffraction (XRD) was investigated by Bruker D8 Advance using Cu K α irradiation at $2\theta=20^\circ$ to 80° with 0.05°s^{-1} step size. The character peak was calculated to define crystallite size by Scherrer's equation.

3.4.4 NH₃-temperature programmed desorption

The acidity of catalysts was performed by the NH₃-TPD technique using Chemisorb 2750 (Micromeritics). The 0.05g powder of catalyst was pretreated to

eliminate moisture and other contaminants at 350°C in the He gas for 1 hour before cooling down to surrounding temperature. Next, the NH₃ adsorption on the surface catalyst was carried out by injecting the 25ml/min of 15% NH₃ in He gas for 1 hour. Then, the system was purged with the gas for removing the excess NH₃. Finally, the desorption of NH₃ can be performed by heating the system by the heating rate of 10°C /min from 30°C to 700°C, and the TCD signal was recorded.

3.4.5 X-ray photoelectron spectroscopy (XPS)

To consider the composition of each element, the catalyst can be analyzed by X-ray photoelectron spectroscopy using Amicus photoelectron spectrometer with Mg K α X-ray source at 20 mA and 10 eV with the C 1s binding energy of 284.6 eV

3.4.6 CO-pulse chemisorption

The dispersion and active metal sites were calculated from the CO-pulse chemisorption technique by Micromeritics ChemiSorb 2750 and ASAP 2101C V.3.00 software. Firstly, the catalyst was pretreated for 1 hour before was reduced under H₂/He flow for 30 min at 450 °C. After that, the system has decreased the temperature for CO adsorption which the 20 μ L of CO gas was injected into the system until saturated. From the calculation, the CO adsorbed/Pt atom is assumed to 1.

3.4.7 Thermogravimetric analysis (TGA)

The catalytic deactivation by coke formation during glycerol hydrogenolysis can be determined via the TPO curve using the thermogravimetric analysis (TGA) technique. The weight loss used catalysts, including coke and other adsorbed species, were measured under temperature program from 25°C to 1000°C with ramp rate of 10°C /min using N₂ UHP as a carrier gas.

3.4.8 Inductively coupled plasma (ICP)

The catalytic deactivation by leaching of Pt and W from the surface catalyst during glycerol hydrogenolysis can be determined via the Inductively coupled plasma by optical emission spectrometry (ICP-OES-2100 DV from Perkin Elmer).



CHAPTER IV

RESULTS AND DISCUSSION

4.1 Physical Appearance

The physical appearance of the fresh catalysts is shown in figure 14. The picture shows all of the fresh catalysts as a fine powder. For Pt/WO_x/γ-Al₂O₃ catalyst, the textural has a fine gray powder. The color of the catalyst was changed from gray to black powder after the third metal was added.

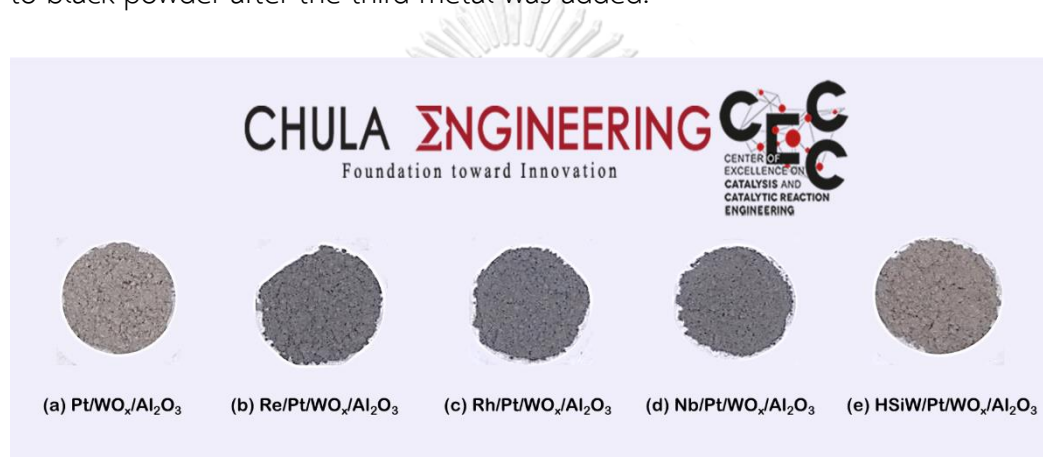


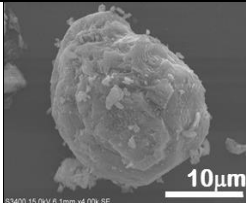
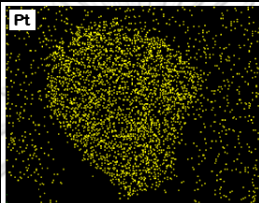
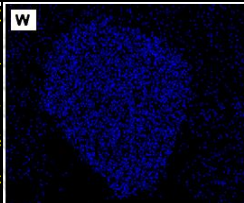
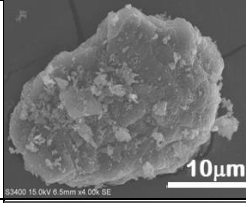
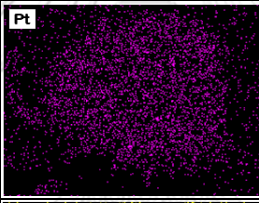
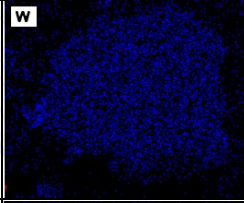
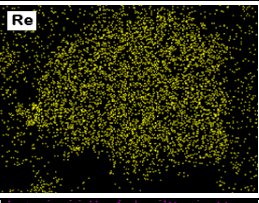
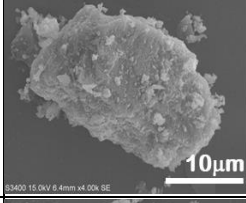
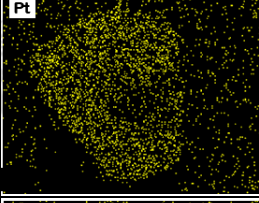
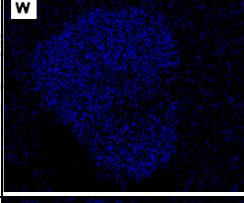
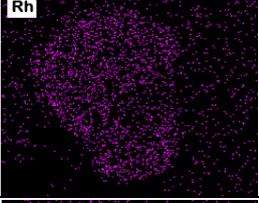
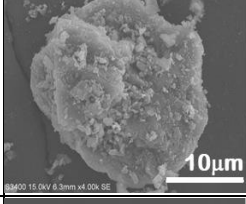
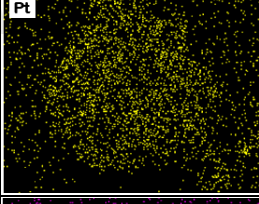
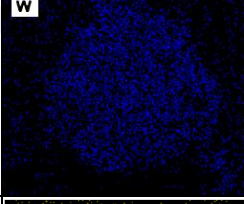
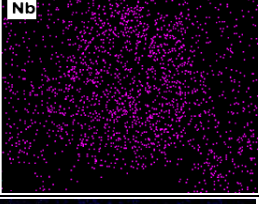
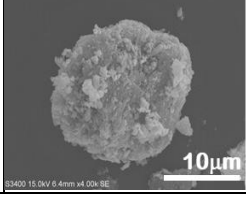
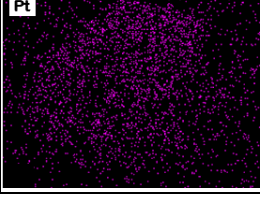
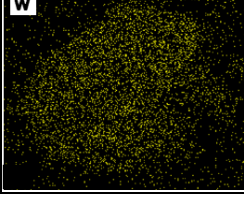
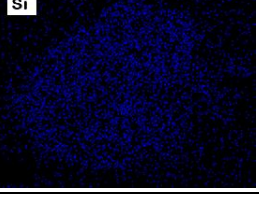
Figure 14 Physical Appearance of fresh catalyst (a) Pt/WO_x/γ-Al₂O₃ (b) Re/Pt/WO_x/γ-Al₂O₃ (c) Rh/Pt/WO_x/γ-Al₂O₃ (d) Nb/Pt/WO_x/γ-Al₂O₃ and (e) HSiW/Pt/WO_x/γ-Al₂O₃

4.2 Morphological properties of the catalyst

The morphological properties of catalysts are analyzed by the SEM-EDX technique, as summarized in Table 5. The morphology structure of the catalyst, including SEM image and EDX mapping of Pt, W, and M metal elements, is extended. Overall, the SEM images of Pt/WO_x/γ-Al₂O₃ catalyst and M dope on Pt/WO_x/γ-Al₂O₃ catalyst by M presenting Re, Rh, Nb, and HSiW, shows similar particles size. Moreover, the metal dispersions of Pt and WO_x on the surface Pt/WO_x/γ-Al₂O₃ catalyst have also presented a uniform with a high dispersion particle size as yellow and blue dot respectively and no detection of Pt accumulation as illustrated by EDX mapping images. Additionally, EDX mapping images of the catalyst after M metals doping also show high dispersion and still maintain Pt and WO_x dispersion. These results indicate

that the M metal doping does not influence the Pt and WO_x aggregation. Therefore, the high distribution of Pt and WO_x on alumina support might remain the metal surface area of catalyst for hydrogenolysis reaction that M/Pt/ $\text{WO}_x/\gamma\text{-Al}_2\text{O}_3$ catalyst performance should be the same or better than that of Pt/ $\text{WO}_x/\gamma\text{-Al}_2\text{O}_3$ catalyst.

Table 5 SEM image and EDX mapping of Pt/ $\text{WO}_x/\gamma\text{-Al}_2\text{O}_3$ catalyst and M/ Pt/ $\text{WO}_x/\gamma\text{-Al}_2\text{O}_3$ catalyst

Catalysts	SEM image ^a	Pt metal ^b	W metal ^c	The third metal ^d
Pt/ $\text{WO}_x/\text{Al}_2\text{O}_3$				n/a
Re/Pt/ $\text{WO}_x/\text{Al}_2\text{O}_3$				
Rh/Pt/ $\text{WO}_x/\text{Al}_2\text{O}_3$				
Nb/Pt/ $\text{WO}_x/\text{Al}_2\text{O}_3$				
HSiW/Pt/ $\text{WO}_x/\text{Al}_2\text{O}_3$				

^a SEM images of fresh Pt/ $\text{WO}_x/\gamma\text{-Al}_2\text{O}_3$ and M/ Pt/ $\text{WO}_x/\gamma\text{-Al}_2\text{O}_3$ catalyst

^b The EDX mapping of Pt element for Pt/ $\text{WO}_x/\text{Al}_2\text{O}_3$ and M/ Pt/ $\text{WO}_x/\gamma\text{-Al}_2\text{O}_3$ catalyst

^c The EDX mapping of W element for Pt/ $\text{WO}_x/\gamma\text{-Al}_2\text{O}_3$ and M/ Pt/ $\text{WO}_x/\gamma\text{-Al}_2\text{O}_3$ catalyst

^d The EDX mapping of M element as a Re, Rh, Nb, and Si for Pt/WO_x/γ-Al₂O₃ and M/ Pt/WO_x/γ-Al₂O₃ catalyst

n/a = non-analysis

Investigation of the composition of elements, SEM technic equipped with EDX mode was considered the composition of Pt and W element. The catalysts preparation was desired from the calculation consist of 0.1 wt.% of the third metals, 5 wt.% of Pt, and 10 wt.% of W by total catalyst weight. The actual element composition of the prepared catalysts is shown in table 7. The results show about 5 wt.% of Pt for all catalysts. Additionally, the W element also shows the percent by weight around 10 wt.%. For the third metal, the results can not detect because only 0.1wt.% was doped. Therefore, the results illustrate that the prepared catalysts via the wet impregnation method correspond to the preparation method's calculation.

Table 6 The composition elements of Pt/WO_x/γ-Al₂O₃ catalyst and M/ Pt/WO_x/γ-Al₂O₃ catalyst analyzed by SEM equipped EDX mode

Catalyst	Composition	
	Pt (wt.%)	W (wt.%)
Pt/WO _x /γ-Al ₂ O ₃	5.8±1.0	11.3±0.8
Re/Pt/WO _x /γ-Al ₂ O ₃	5.0±1.0	12.2±0.3
Rh/Pt/WO _x /γ-Al ₂ O ₃	5.1±0.9	10.9±0.7
Nb/Pt/WO _x /γ-Al ₂ O ₃	4.9±0.1	12.5±0.7
HSiW/Pt/WO _x /γ-Al ₂ O ₃	5.0±0.4	11.1±0.7

Other morphological properties of the catalyst are the surface area properties analyzed via the N₂-Physisorption technic using the Brunauer-Emmett-Teller (BET) equation. Table 7 are concluded the surface properties consist of BET surface area, pore size, and pore volume. The BET surface area of the catalysts after Re and Rh doped on the Pt/WO_x/γ-Al₂O₃ catalyst are similar. Additionally, the pore size of the catalysts does not change. Although the surface drops from 63.0 m²g⁻¹ to 34.3 m²g⁻¹ due to the high amount of dopant for HSiW/Pt/WO_x/γ-Al₂O₃, the pore structure is not disrupted. For Nb on Pt/WO_x/γ-Al₂O₃ catalyst, the BET surface area of the catalyst is significantly increased, but the pore size of the catalyst is decreased. It can be concluded that the effect of the third metal maintains the surface structure of Pt/WO_x/γ-Al₂O₃ catalyst after Re and Rh doping as a promoter on Pt/WO_x/γ-Al₂O₃ catalyst but the Nb metal influence the surface structure of Pt/WO_x/γ-Al₂O₃ catalyst due to it may be affected to pore blockage on the surface catalyst. However, the increment of surface area after Nb-doped, needs to be more discussed.

The CO-chemisorption technique analyses the metal surface properties of fresh catalysts, as shown in table 7. The fresh Pt/WO_x/γ-Al₂O₃ catalyst provides 20.2 m²g_{metal}⁻¹ of metal surface with 8.2% metal dispersion. The metal surface of fresh catalysts increases from 20.2 m²g_{metal}⁻¹ to 27.0, 30.3, 30.2, and 29.0 m²g_{metal}⁻¹ when Re, Rh, Nb, and HSiW promoter is doped into Pt/WO_x/γ-Al₂O₃ catalyst, respectively that resulting in the metal dispersion on the surface catalyst. Moreover, the metal size was calculated by CO-chemisorption technic in table 7 that shows the decreased metal size after dope the third metal. It could be reasoned that the metal surface area increases due to better dispersion of metal that can provide more metal active sites for hydrogenolysis reaction resulted in decreased metal size on the catalyst surface. Therefore, the third metal-doped on Pt/WO_x/γ-Al₂O₃ catalyst may improve the catalytic efficiency better than Pt/WO_x/γ-Al₂O₃ catalyst discussed in the next section. Moreover, the metal size of the fresh catalyst is determined by CO-chemisorption. The metal size of the M/Pt/WO_x/γ-Al₂O₃ catalyst is smaller than

Pt/WO_x/γ-Al₂O₃ catalyst. Therefore, it can be concluded that the added the third metal effect to decrease the metal size of the catalyst.



Table 7 The N₂-Physisorption of Pt/WO_x/γ-Al₂O₃ catalyst and M/Pt/WO_x/γ-Al₂O₃ catalyst using BET analysis

Catalyst	Surface Area (m ² g ⁻¹)	Pore Size (nm)	Pore Volume (cm ³ /g)	^a Metal surface		^a Metal size (nm)
				area (m ² g _{metal} ⁻¹)	dispersion (%)	
Pt/WO _x /γ-Al ₂ O ₃	63.0	9.0	0.14	20.2	8.2	14.1
Re/Pt/WO _x /γ-Al ₂ O ₃	70.0	8.4	0.14	27.0	10.9	10.6
Rh/Pt/WO _x /γ-Al ₂ O ₃	62.8	8.8	0.14	30.3	12.3	9.4
Nb/Pt/WO _x /γ-Al ₂ O ₃	n/d	n/d	n/d	30.2	12.2	9.4
HSW/Pt/WO _x /γ-Al ₂ O ₃	34.3	12.0	0.10	29.0	11.7	9.8

^a The metal surface properties using CO-chemisorption technic

n/d = not determine

4.3 Effect of the third metal on Pt/WO_x/γ-Al₂O₃ catalyst under hydrogenolysis of glycerol

The glycerol hydrogenolysis test was performed under 140°C and 20 bar of initial hydrogen pressure for 6 hours as previously chapter. The activity of fresh Pt/WO_x/γ-Al₂O₃ catalyst and M/Pt/WO_x/γ-Al₂O₃ catalyst under glycerol hydrogenolysis reaction and crucial information of %conversion and %selectivity of wanted 1,3PDO and undesired byproducts including 1,2PDO, 1-PrOH, and 2-PrOH is shown in Table 8. The result indicates glycerol conversion of Pt/WO_x/γ-Al₂O₃ as a mother catalyst is 36.4%, while selectivity of wanted 1,3-propanediol is 29.6%. In comparison, the glycerol conversion of catalysts is significantly increased from 36.4% to 48.8%, 49.3%, 52.6%, and 49.3% when Re, Rh, Nb, and HSiW metal was doped on Pt/WO_x/γ-Al₂O₃ catalyst, respectively. The M/Pt/WO_x/γ-Al₂O₃ catalyst promotes better activity in terms of glycerol conversion.

Interestingly, the Re doped on Pt/WO_x/γ-Al₂O₃ catalyst represents the best catalyst in terms of 1,3-propanediol production. It could be reasoned that the increment of catalytic activity by doping of the third metal into Pt/WO_x/γ-Al₂O₃ catalyst can improve the catalytic performance in terms of glycerol conversion and selectivity of 1,3PDO production as well as retarding unwanted by-products because the third metal can promote the better dispersion of metal on the surface catalyst that provides high metal surface area for reaction supporting with CO-chemisorption result that mentioned previously section. Additionally, the Re metal also illustrated the best promoter to produce 1,3-propanediol due to increased acidity.

Table 8 The activity of Fresh of Pt/WO_x/γ-Al₂O₃ catalyst and M/ Pt/WO_x/γ-Al₂O₃ catalyst in glycerol hydrogenolysis reaction under reaction conditions: 140°C and 20 bar of initial hydrogen pressure for 6 hours of reaction time

Catalyst	Glycerol conversion (%)	Selectivity (%)				1,3PDO yield (%)	C ₃ liquid/Gas mass ratio	C ₃ mass balance (%)
		1,3-PDO	1,2-PDO	1-PrOH	2-PrOH			
Pt/WO _x /Al ₂ O ₃	36.4±2.6	29.6±1.7	23.1±0.1	6.2±0.2	10.3±0.7	10.8	0.837	83.7
Re/Pt/WO _x /Al ₂ O ₃	48.8±0.4	43.1±0.7	19.5±0.0	9.0±1.4	19.0±0.0	21.0	0.889	88.9
Rh/Pt/WO _x /Al ₂ O ₃	49.3±0.4	28.2±0.7	17.7±0.0	5.7±1.4	11.7±0.0	13.9	0.765	76.5
Nb/Pt/WO _x /Al ₂ O ₃	49.8±0.6	27.9±2.4	18.3±0.4	9.4±2.5	5.3±0.9	13.9	0.733	73.4
HSW/Pt/WO _x /Al ₂ O ₃	49.3±0.4	24.4±5.8	17.9±0.2	4.7±0.3	8.3±1.8	12.0	0.765	76.5

4.3 Effect of the third metal on catalytic stability

Although the existence of the third metal can promote the catalytic activity and selectivity to transform glycerol to be 1,3-propanediol, however, the stability of the catalyst is also the indispensable factor to design the new better catalyst for the industry. In this section, the catalytic stability of the Pt/WO_x/γ-Al₂O₃ catalyst and the third metal doping on Pt/WO_x/γ-Al₂O₃ catalyst in terms of glycerol conversion of fresh catalyst comparing with used catalyst are investigated. Figure 15 illustrate the catalytic stability in term of fresh catalyst comparing with used catalyst under glycerol hydrogenolysis reaction to produce 1,3-propanediol. For Pt/WO_x/γ-Al₂O₃ catalyst, the glycerol conversion decreases from 36.4% to 17.8%, with 51.1% of deactivation. Interestingly, the glycerol conversion of Re and Rh metal doping on Pt/WO_x/γ-Al₂O₃ catalysts are slightly decreased from 48.8% to 46.8% and 49.3% to 41.2% with 4.1% and 16.1% of deactivation, respectively. However, the result shows a greatly dropped in conversion after the Nb metal was doped on Pt/WO_x/γ-Al₂O₃ catalyst. Therefore, It could be concluded that the Re and Rh as a third metal not only promote the activity and selectivity of catalyst but also improve stability of Pt/WO_x/γ-Al₂O₃ catalyst on reused for hydrogenolysis reaction of glycerol. Although the Nb metal can increase the catalyst activity, the stability of the catalyst is needed. As a result, the worse catalyst stability may occur from the deactivation of catalysts for many reasons: coke formation, the sintering of the active site, and leaching of the active site. So, the deactivation of the catalyst during the hydrogenolysis of glycerol reaction will be discussed in the next section.

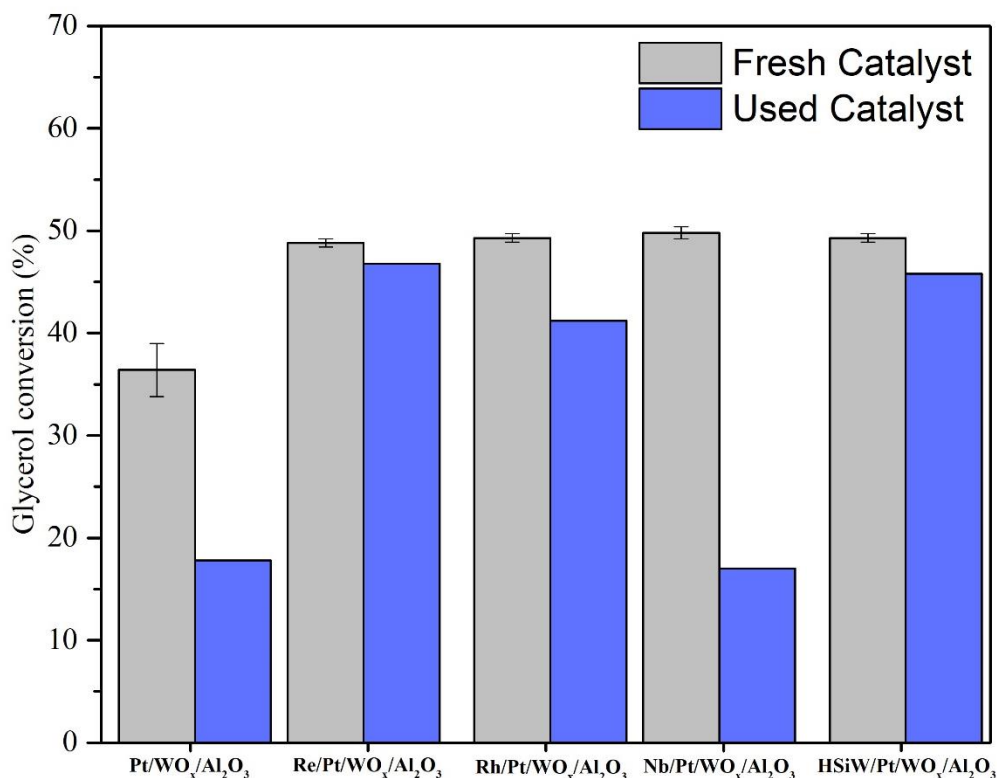


Figure 15 Catalytic stability in terms of fresh catalyst comparing used catalyst under hydrogenolysis reaction

4.4 Effect of the third metal on Pt/WO_x/γ-Al₂O₃ catalyst for deactivation of the catalyst

In this section, the deactivation of the catalyst is investigated which the hydrogenolysis reaction is hydrothermal reaction was under liquid phase. Therefore, the main deactivation for this process is metal leaching, sintering, and coking these are considered to explain the deactivation of catalyst in this process [42].

To investigate the deactivation of the catalyst, the surface properties of fresh and used catalysts during glycerol hydrogenolysis were examined by N₂-physisorption and CO-chemisorption technique concluded in Table 3, as well as the percent deactivation in term glycerol conversion. The physical surface area of catalyst analyzed by N₂-physisorption was decreased with all of the catalyst comparing with the used catalyst after the second round of glycerol hydrogenolysis. Additionally, the metal surface properties of the fresh comparing with reused catalyst were included

using the CO-chemisorption technique. For the fresh and reused Pt/WO_x/γ-Al₂O₃ catalyst, metal surface area, and metal dispersion were decreased from 20.2 m²g_{metal}⁻¹ to 10.2 m²g_{metal}⁻¹ and 8.2% to 4.1% respectively while the 51.1% deactivation of the first round hydrogenolysis of glycerol comparing with reused catalyst as a second-round hydrogenolysis reaction was obtained.

Interestingly, the metal surface area and metal dispersion of reused catalyst for Re and Rh as a promoter doped on Pt/WO_x/γ-Al₂O₃ catalyst were slightly changed comparing with Pt/WO_x/γ-Al₂O₃ catalyst resulting in retarding deactivation of the catalyst. This indicated that the loss of metal surface area through metal dispersion affected a significant role in catalytic performance in terms of glycerol conversion. As a result, the loss of metal surface area through metal dispersion may be related to metal leaching, metal sintering, and coking causing the deactivation of catalysts these needed to be discussed. However, the metal surface area analyzed by CO-chemisorption technic cannot calculate metal sintering because the decreased metal surface area analyzed by CO-chemisorption technic may occur from loss of Pt active site via catalyst deactivation from metal sintering, metal leaching, and coke formation on the metal surface [42].

Table 9 Surface properties of fresh and used catalysts on deactivation of the catalyst

Catalyst	Catalytic cycle	Surface area (m ² g ⁻¹)	Metal surface area (m ² g _{metal} ⁻¹)	Metal dispersion (%)	^a Deactivation (%)
Pt/WO _x /Al ₂ O ₃	Fresh	63.0	20.2	8.2	51.1
	Used	50.5	10.2	4.1	
Re/Pt/WO _x /Al ₂ O ₃	Fresh	69.9	27.0	10.9	4.1
	Used	48.9	23.8	9.6	
Rh/Pt/WO _x /Al ₂ O ₃	Fresh	62.8	30.3	12.3	16.4
	Used	47.2	26.6	10.8	

Nb/Pt/WO _x /Al ₂ O ₃	Fresh	n/d	30.2	12.2	65.9
	Used	n/d	2.1	0.9	
HSiW/Pt/WO _x /Al ₂ O ₃	Fresh	34.3	39.0	11.7	8.3
	Used	42.5	27.1	10.6	

^aThe deactivation percent of catalyst calculated by glycerol conversion of fresh catalyst comparing with used catalyst

n/d = not determine

4.4.1 Effect of the third metal on metal sintering

The stability of the catalyst was performed under hydrogenolysis of glycerol that the catalyst after the first cycle was tested as second-round glycerol hydrogenolysis. The result illustrated the deactivation of catalyst was decreased when Re, Rh, and HSiW were added. To study the effect of the third metal on stability, the deactivation of catalyst from metal sintering, metal leaching, and coking are investigated. Firstly, the metal sintering was investigated using the XRD technique to identify Pt crystallite size. The XRD patterns of fresh catalyst comparing with used catalyst are plotted as shown in Figure 16. For all catalysts, the diffraction peaks at 39.9°, 46.4°, and 67.5° were Pt (111), (200) and (220) reflections respectively [43-45], while the peaks refer to γ -Al₂O₃ have reported at 37.5°, 45.5°, and 67.0° [46]. For the m-WO₃ were not illustrated in this study, that can be reported high WO_x species dispersion on γ -Al₂O₃ support [47]. On the used catalyst, the result presents characteristic diffraction peaks of Pt at 39.9° for used Pt/WO_x/ γ -Al₂O₃ and used M/Pt/WO_x/ γ -Al₂O₃ catalyst obviously increased intensity indicated the growth of Pt atom. Therefore, the catalyst has deactivation from Pt sintering after the glycerol hydrogenolysis.

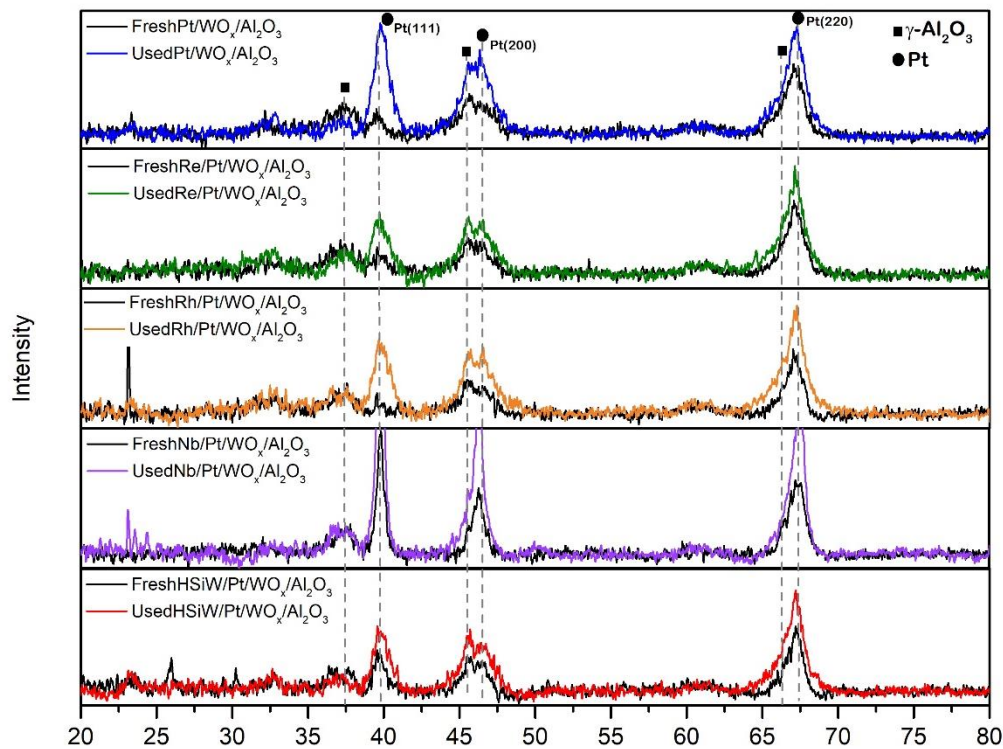


Figure 16 XRD patterns of fresh and used Pt/WO_x/γ-Al₂O₃ and M/Pt/WO_x/γ-Al₂O₃ catalyst (M represent Re, Rh, Nb, and HSiW)

The Pt metal crystallite size can be examined for the characteristic diffraction peaks at 39.9° by XRD using the Scherrer equation as shown in equation (1).

$$\text{Pt metal crystallite size (nm)} = \frac{K\lambda}{\beta \cos\theta} \quad (1)$$

Where K is Scherrer's constant take as 0.9 for good approximation, λ is the X-ray wavelength, which is equal to 0.154 nm, β is the full width at half maximum (FWHM) at θ in radians unit, and θ is characteristic diffraction peaks of Pt from XRD pattern in radians unit [48].

For fresh Pt/WO_x/γ-Al₂O₃, Re/Pt/WO_x/γ-Al₂O₃, Rh/Pt/WO_x/γ-Al₂O₃, and HSiW/Pt/WO_x/γ-Al₂O₃ catalyst, the Pt metal crystallite size are 10.6, 9.9, 10.1, and 12.6 nm respectively as shown in Table 10. Moreover, the used Pt/WO_x/γ-Al₂O₃

catalyst has the growth of Pt atom to 14.7 nm with 38.2% of Pt sintering. Interestingly, the Re, Rh, and HSiW as a promoter can decrease the growth of Pt atom resulting retarding the deactivation of catalyst from Pt sintering. However, to identify Pt metal crystallite size by XRD using the Scherrer equation is a limitation for Nb/Pt/WO_x/γ-Al₂O₃ catalyst because the Pt crystallite size may be too small that is a limitation for the XRD technique and the property of Nb element. Therefore, it should be studied by another characterization.

Table 10 The Pt metal crystallite size for fresh and used catalyst and the sintering of Pt metal crystallite size after hydrogenolysis reaction

Catalyst	Catalytic cycle	Pt metal crystallite size ^a (nm)	Pt Sintering (%)
Pt/WO _x /Al ₂ O ₃	Fresh	10.6	38.2
	Used	14.7	
Re/Pt/WO _x /Al ₂ O ₃	Fresh	9.9	14.6
	Used	11.4	
Rh/Pt/WO _x /Al ₂ O ₃	Fresh	10.1	12.5
	Used	11.3	
Nb/Pt/WO _x /Al ₂ O ₃	Fresh	n/d	n/d
	Used	n/d	
HSiW/Pt/WO _x /Al ₂ O ₃	Fresh	12.6	3.6
	Used	13.0	

^a Pt metal crystallite size determined by XRD using the Scherrer equation

From the literature review, the formation of metal-metal bonding on the surface catalyst can change in the electronic, chemical, and catalytic properties of metal catalyst which the electronegativity value of the third metal as a promoter has been investigated in this study [26].

The semi-log plot between Pt sintering (%) and difference of electronegativity value (ΔEN) calculated by electronegativity value of the third metal minus electronegativity value of Pt metal is showed in Figure 17. The data illustrated the higher difference of electronegativity value comparing with Pt can reduce the Pt sintering as a correlation Pt sintering (%) equal to $15.646e^{-3.786\Delta EN}$. So, it can be concluded that the deactivation of catalyst from Pt sintering does not depend on the third metal but relate to the electronegativity value of the third metal and this model is proved by Zn as the third metal.

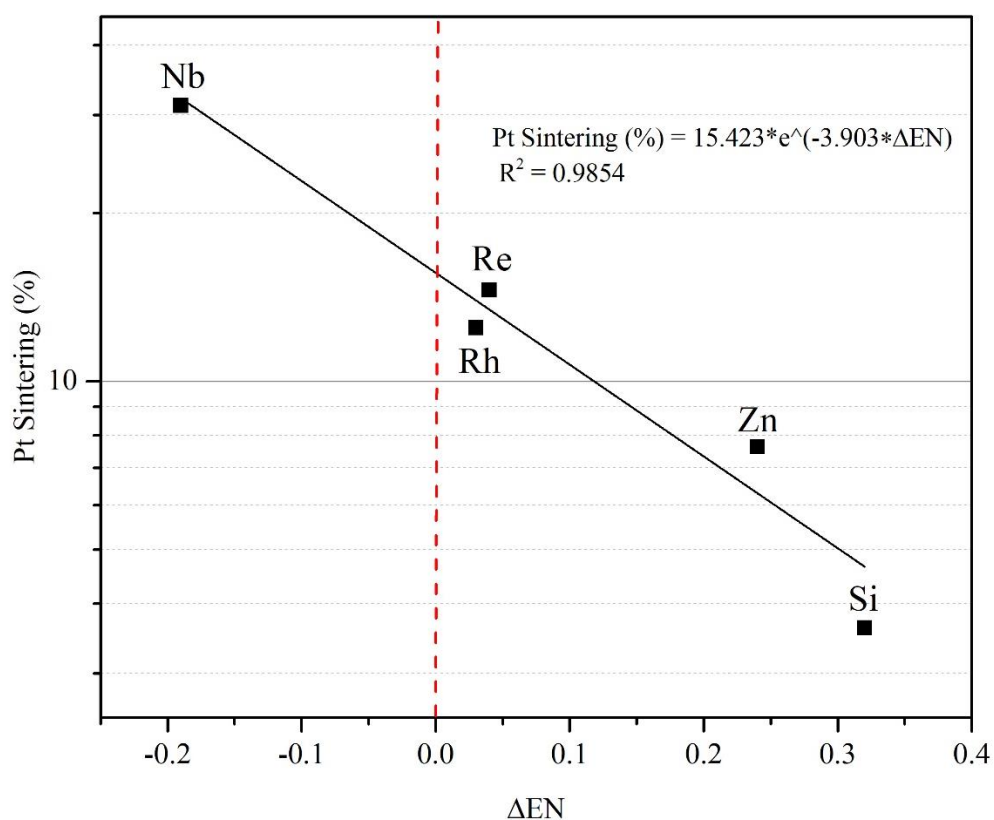


Figure 17 The semi-log graph between Pt sintering (%) and difference of electronegativity value (ΔEN)

4.4.2 Effect of the third metal on metal leaching

Due to the liquid phase hydrogenolysis and hydrothermal reaction, leaching of the metal particles has normally been investigated to be another major factor of deactivation mechanisms for aqueous phase reaction.

The metal leaching was studied by the amount of Pt and W leaching from the surface of the catalyst in an aqueous phase reaction using ICP-EOS analysis. The amount of metal leaching consist of Pt and W metal is presented in Table 11. For Pt/WO_x/γ-Al₂O₃ catalyst, 0.08% of Pt leaching was obtained after the first round of hydrogenolysis reaction. Moreover, Increment of Pt leaching was found to 0.18% of Pt leaching when Nb was added. Attractively, the Pt leaching was not detected in aqueous phase reaction after Re, Rh, and HSiW as a promoter on Pt/WO_x/γ-Al₂O₃ catalyst. However, the results also show the leaching of W in contrast with Pt leaching.

Table 11 Metal leaching from surface of catalyst to aqueous phase reaction (Leaching of Pt and W) using ICP-EOS analysis

Catalyst	Pt leaching (%)	W leaching (%)
Pt/WO _x /Al ₂ O ₃	0.08	0.27
Re/Pt/WO _x /Al ₂ O ₃	0.00	0.14
Rh/Pt/WO _x /Al ₂ O ₃	0.00	0.35
Nb/Pt/WO _x /Al ₂ O ₃	0.18	0.08
HSiW/Pt/WO _x /Al ₂ O ₃	0.00	8.49

As mentioned in the previous section, the electronegativity value of the third metal is an independent variable for Pt sintering effect. Therefore, the electronegativity value of the third metal is investigated for the metal leaching effect. The relation between Pt leaching (%) and difference of electronegativity value of the third metal comparing with Pt (ΔEN) are shown in Figure 18. Interestingly, the Pt

leaching was not detected for the third metal which has more electronegativity value than Pt metal indicates that the suppression of Pt leaching requires a higher electronegativity value of the third metal than Pt metal for promoting on Pt/WO_x/γ-Al₂O₃ catalyst.

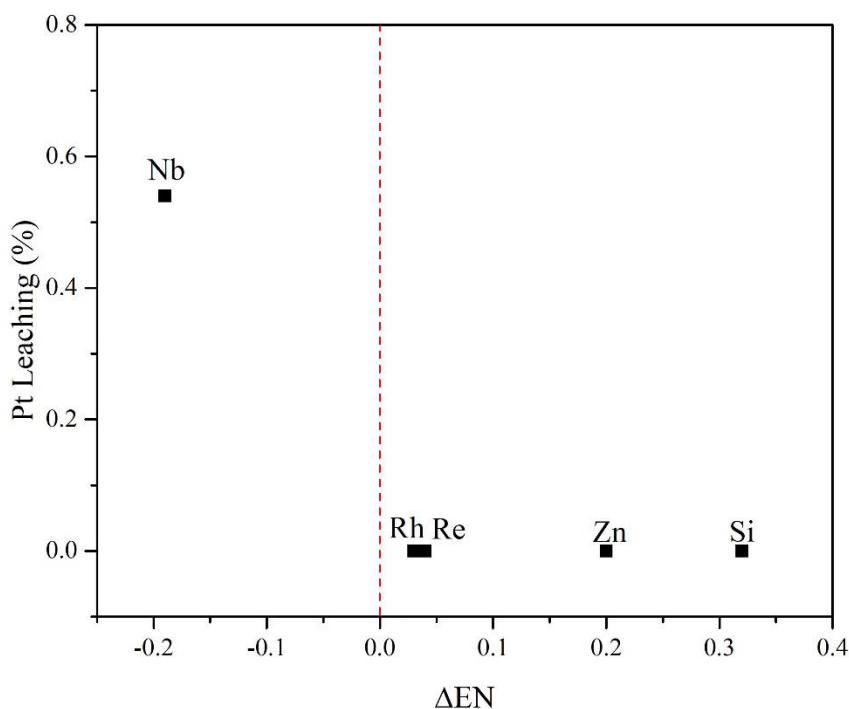


Figure 18 The correlation between Pt leaching (%) and difference of electronegativity value (ΔEN)

Additionally, the relation between W leaching (%) and the difference of electronegativity value of the third metal comparing with Pt (ΔEN) are also shown in Figure 19. The graph illustrates the increasing electronegativity value of the third metal enhances the W leaching. Therefore, the deactivation of catalyst from metal leaching can be concluded that the higher EN value of the third metal comparing with Pt can suppress the Pt leaching in contrast it increases the W leaching. This suggested that the loss of Pt active site via leaching plays the role in the stability of catalyst in term glycerol conversion as the mentioned previous section.

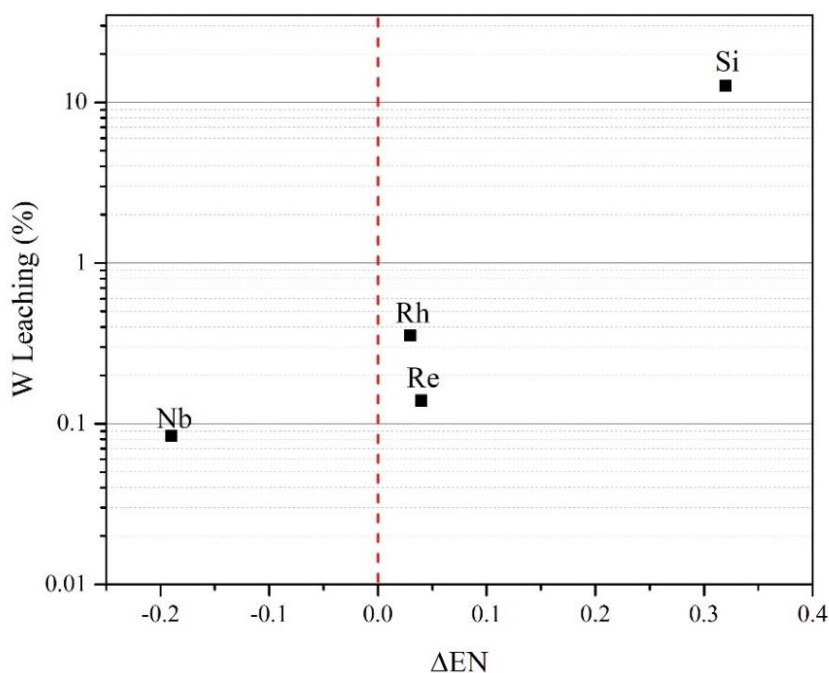


Figure 19 The correlation between W leaching (%) and difference of electronegativity value (ΔEN)

From the literature review, investigate the effect of electronegativity value of metal-metal in the bimetallic surface that affect the electron transfer. In this study, for the third metal that has a higher electronegativity value than Pt metal such as Re, Rh, and HSiW, the Pt metal play the role of electron donor to the third metal provides the positive charge on Pt. Therefore, the charge was balanced by electron transfer from Al_2O_3 support to Pt metal resulting in stronger interaction between Pt with oxygen on Al_2O_3 support. The stronger interaction of Pt metal on support suggesting the suppression of Pt leaching and reduced Pt sintering, while metal that has lower electronegativity value than Pt metal such as Nb, the Pt metal play the roles for electron acceptor from the third metal provide the negative charge by a high electron density surrounded Pt metal these affect to weaker interaction between Pt with Al_2O_3 support resulting to enhanced Pt leaching and sintering after doped Nb on $Pt/WO_x/\gamma-Al_2O_3$ catalyst. Moreover, the negative charge by a high

electron density surrounded Pt metal effect on the larger size of Pt particles relate to the increased of Pt particles calculated by XRD pattern using Scherrer equation.

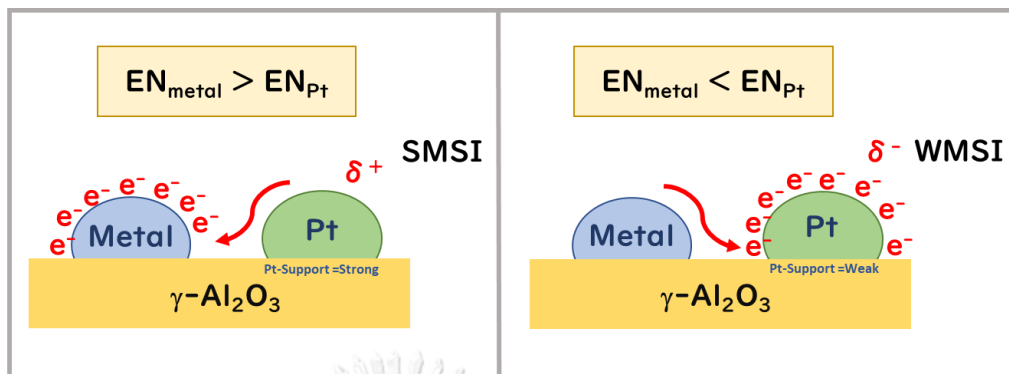


Figure 20 Schematic of Metal-Support interaction

4.4.3 Effect of the third metal on metal-support interaction

Based on the hypothesis that the strong metal-support interaction would reduce the Pt leaching and Pt sintering which the Pt sintering requires a stronger interaction of the metal with support than the Pt leaching for inhibits the agglomeration of Pt on the surface catalyst. Therefore, the effect of the third metal on the metal-support interaction via the surface chemical state of Pt metal is investigated.

To study the effect of promoters on the surface chemical state of an individual element can be determined via the analysis of chemical state analysis using the XPS technique. The chemical state of Pt element in Pt/WO_x/γ-Al₂O₃, Re/Pt/WO_x/γ-Al₂O₃, Rh/Pt/WO_x/γ-Al₂O₃, Nb/Pt/WO_x/γ-Al₂O₃, and HSiW/Pt/WO_x/γ-Al₂O₃ catalysts can be plotted as Pt-4f XPS spectra which are illustrated in Fig.21a, Fig.21b, Fig.21c, Fig.21d, and Fig 21e, respectively. The XPS peaks at a binding energy of 71.6, 72.9, and 75.0 eV indicate Pt-4f_{7/2} of Pt⁰, Pt²⁺, and Pt⁴⁺, respectively. Moreover, the characteristic XPS peaks at 74.9, 76.2, and 77.6 eV can be assigned to Pt-4f_{5/2} of Pt⁰, Pt²⁺, and Pt⁴⁺ respectively [47, 49, 50]. The red peaks as Pt⁰ are notably decrease from 34.7% to 26.7%, 21.1%, and 15.9% when doping Re, Rh, and

HSiW metal on Pt/WO_x/γ-Al₂O₃, respectively. In contrast, decreased Pt⁰ has promoted increased blue peaks that represent Pt²⁺. It can be concluded that the addition of Re, Rh, and HSiW on Pt/WO_x/γ-Al₂O₃ catalyst can increase the oxidation state from Pt⁰ to Pt²⁺. The observed increased concentration of Pt²⁺ reveals the stronger interaction of Pt with oxygen on the Al₂O₃ support which inhibits Pt leaching and leads to high dispersion of Pt on the surface that supports CO-chemisorption. Besides, the green peaks correspond to Pt⁴⁺ are not change for Pt/WO_x/γ-Al₂O₃, Re/Pt/WO_x/γ-Al₂O₃, and Rh/Pt/WO_x/γ-Al₂O₃ catalyst. However, green peaks as Pt⁴⁺ in HSiW/Pt/WO_x/γ-Al₂O₃ catalysts are increased from 35.2% to 44.3%. The results indicate that the oxidation state not only changes from Pt⁰ to Pt²⁺ but also increased the state of Pt⁴⁺ stronger than Pt²⁺ reveals tighter interaction of Pt with oxygen on the Al₂O₃ support which may be reduced Pt sintering as required tighter interaction of Pt and support than Pt leaching.

In the case when the Nb promoter was added into Pt/WO_x/γ-Al₂O₃ catalyst, the red peaks as Pt⁰ are increasing from 34.7% to 51.2% which the increment of Pt⁰ affects to decreased Pt²⁺ from 30.1% to 21.3%. However, the peaks of Pt⁴⁺ were not significantly changed. The observed decrease of Pt²⁺ peak refers to the oxidation state not only change from Pt²⁺ to Pt⁰ resulting in weaker interaction between Pt metal and Al₂O₃ support these indicate that increase of Pt leaching and sintering.

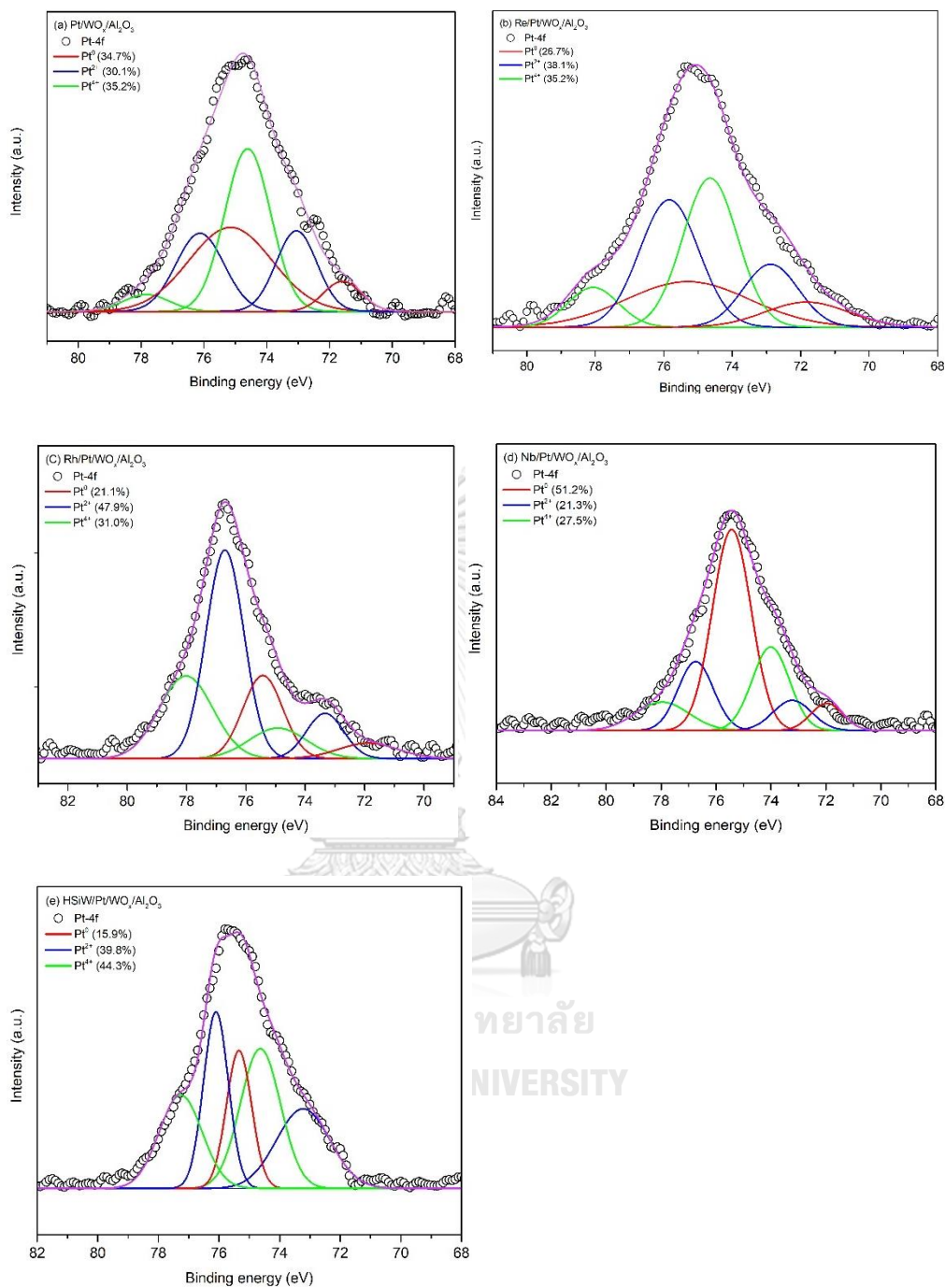


Figure 21 XPS spectra of Pt-4f for (a). Pt/WO_x/Al₂O₃ and (b). Re/Pt/WO_x/Al₂O₃ (c). Rh/Pt/WO_x/Al₂O₃ (d). Nb/Pt/WO_x/Al₂O₃ (e). HSiW/Pt/WO_x/Al₂O₃. Note that the red, blue, and green peaks are represented to Pt⁰, Pt²⁺, and Pt⁴⁺ respectively

4.4.3 Effect of the third metal dope on coke formation

In this section, the deactivation of the catalyst during glycerol hydrogenolysis due to coke formation since the hydrothermal reaction is described. To measure coke formation on the catalyst surfaces, TPO curves of Pt/WO_x/γ-Al₂O₃ and M/Pt/WO_x/γ-Al₂O₃ catalysts are plotted in Fig.22. The amount of total coke that forms during the reaction and the types of coke are characterized in Table12. According to the result, the presence of M metal on Pt/WO_x/γ-Al₂O₃ catalyst displays less amount of total coke than Pt/WO_x/γ-Al₂O₃ catalyst. Therefore, the addition of M increases the catalyst activity and decreases the amount of coke formation. Additionally, coke formation on both Pt/WO_x/γ-Al₂O₃ and M/Pt/WO_x/γ-Al₂O₃ catalyst exhibits two types. The first type is a soft coke that the TPO peak appears in the range of 200 to 400°C called “Type I”. The second type is a hard coke that the TPO peak appears in the range of 400 to 550°C. The soft coke which is more reactive to oxygen appears at the low temperature of the TPO profile which has been indicated to coke on the metallic surface whereas the hard coke can be taken place in the vicinity of the metal-supported interface and the surface support [51] called “Type II”. Additionally, the result shows the coke above 550°C is the coke on a support called “Type III” after Rh and Nb were added.

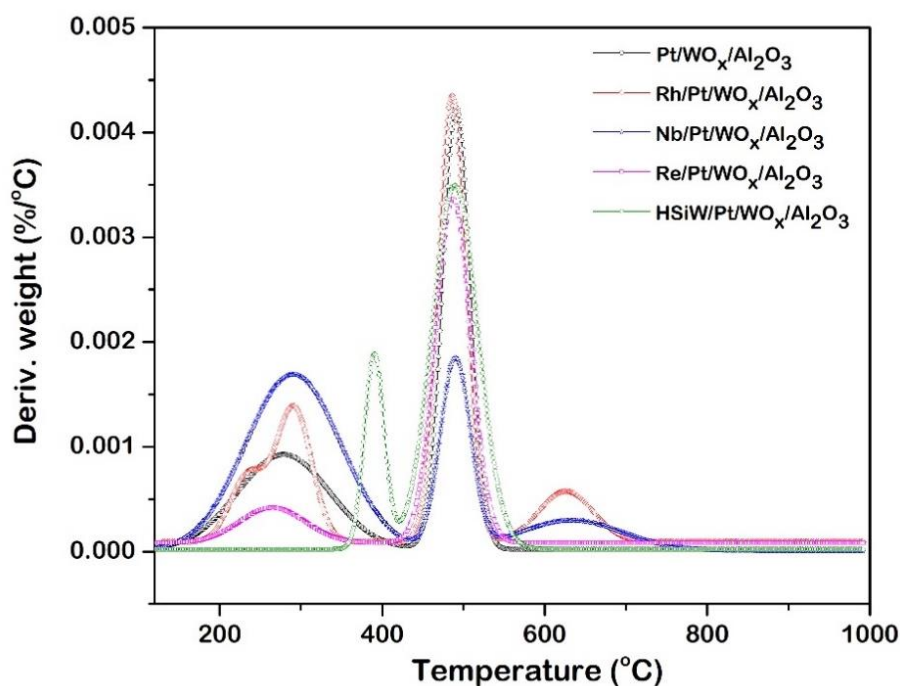


Figure 22 TPO analysis for (a). Pt/WO_x/Al₂O₃ and (b). Re/Pt/WO_x/Al₂O₃ (c). Rh/Pt/WO_x/Al₂O₃ (d). Nb/Pt/WO_x/Al₂O₃ (e). HSiW/Pt/WO_x/Al₂O₃

The total coke and type of coke, analyzed by TGA analysis, are concluded in Table 12 that the amount of total coke for all catalysts is no different. Interestingly, the type coke ratio, type I per type II, is decreased when the Rh, Re, and HSiW as a third metal was added that means the removal of coke on the metal to the support. Additionally, type III of coke occurred when Rh and Nb metal was added. The decreased coke type I refers to removable coke on metal to support resulting maintain the metal site which is the main site for this reaction.

From the result, the Pt/WO_x/γ-Al₂O₃ catalyst contains Type I and Type II. Doping of Re can obviously reduce coke Type I which covers the active site of Pt. Consequently, the activity of Re/Pt/WO_x/γ-Al₂O₃ will not significantly drop although the occurrence of coke formation because Re might play an important role on coke diffusion on Pt active site to the γ-Al₂O₃ support during hydrogenolysis reaction.

Table 12 Total coke formation and type of coke of Pt/WO_x/γ-Al₂O₃ andM/Pt/WO_x/γ-Al₂O₃ catalyst using TGA analysis

Catalyst	Type of coke			Type I /Type II ratio	Total Coke (%)
	Type I (%)	Type II (%)	Type III (%)		
Pt/WO _x /Al ₂ O ₃	43.5	56.5	-	0.77	2.2
Rh/Pt/WO _x /Al ₂ O ₃	31.2	56.3	12.5	0.55	1.9
Nb/Pt/WO _x /Al ₂ O ₃	65.4	22.4	12.2	2.92	1.7
Re/Pt/WO _x /Al ₂ O ₃	15.9	84.1	-	0.19	1.9
HSiW/Pt/WO _x /Al ₂ O ₃	18.6	81.4	-	0.23	1.8

CHAPTER V

CONCLUSION

5.1 Conclusion

The study on the roles of the third metal as a promoter on activity, selectivity, and stability in the Pt/WO_x/γ-Al₂O₃ catalyst during the hydrogenolysis of glycerol can be concluded as follows. On the increased catalytic activity, introducing the third metal on Pt/WO_x/γ-Al₂O₃ catalyst has increases the activity of catalyst comparing with Pt/WO_x/γ-Al₂O₃ catalyst. The improved activity can explain by the increasing metal surface area through higher metal dispersion after the third metal was added. Moreover, the stability of reused catalyst was dropped by more than 50% as found in Pt/WO_x/γ-Al₂O₃ and Nb/Pt/WO_x/γ-Al₂O₃ catalyst, while the Re and Rh doped on Pt/WO_x/γ-Al₂O₃ catalyst show the better stability of the catalyst, which the stability of catalyst directly linked to the loss of metal surface area through deactivation from Pt leaching, Pt sintering, and carbon deposition. For the deactivation of the catalyst, the results suggested the independent variable is the electronegativity of the third metal which higher EN value comparing with Pt can suppress Pt leaching as found in Re, Rh, and HSiW promoter. Moreover, the deactivation of Pt sintering requires much difference of EN value between the third metal and Pt. Due to change of electronic property of Pt after dope, the promoter affects Pt and support interaction, which the XPS result indicates the increased state of Pt⁰ to Pt²⁺ as found in Re, Rh, and HSiW doping that has higher EN value than Pt which suppress the Pt leaching due to the stronger interaction between Pt and γ-Al₂O₃ support, while increased Pt⁴⁺ was found in only HSiW promoter that has a high difference of EN value between the third metal and Pt indicate the tighter interaction between Pt and γ-Al₂O₃ support against Pt agglomeration resulting from reducing Pt sintering. Moreover, the third metal can improve the coke formation by removing the

coke on Pt metal to γ -Al₂O₃ support that can remain the Pt metal as a main active site for hydrogenolysis reaction.

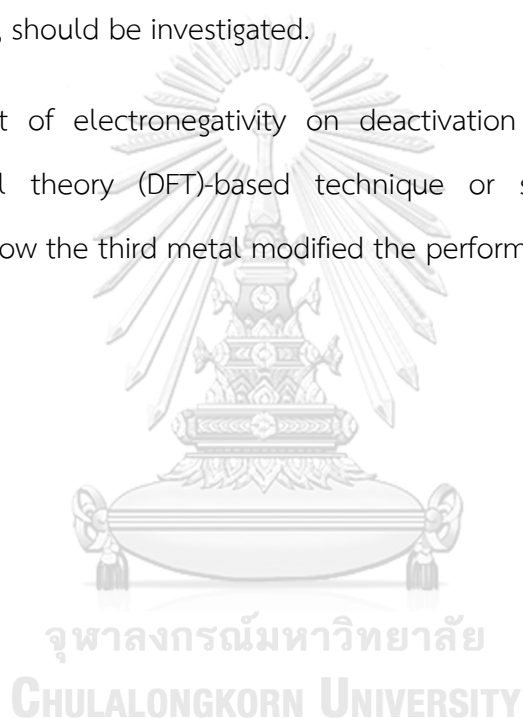
5.2 Recommendations

5.2.1 Py-IR of catalysts should be studied to explain the selective hydrogenolysis to the wanted product.

5.2.2 The physical surface area after Nb-doped, should be studied.

5.2.3 The interaction between the third metal with Pt metal and the third metal with γ -Al₂O₃ should be investigated.

5.2.4 Effect of electronegativity on deactivation should be applied with density functional theory (DFT)-based technique or simulation to study the fundamentals of how the third metal modified the performance of the catalyst.

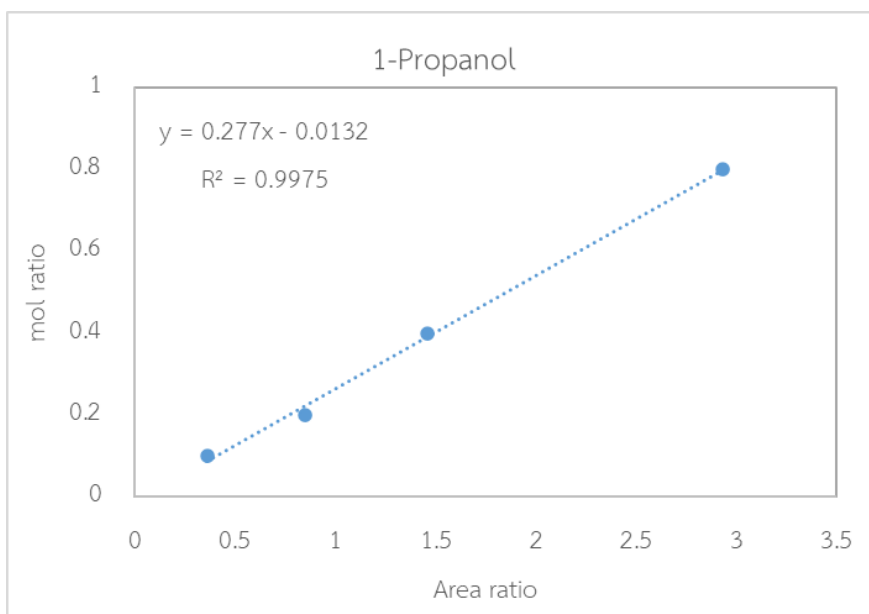




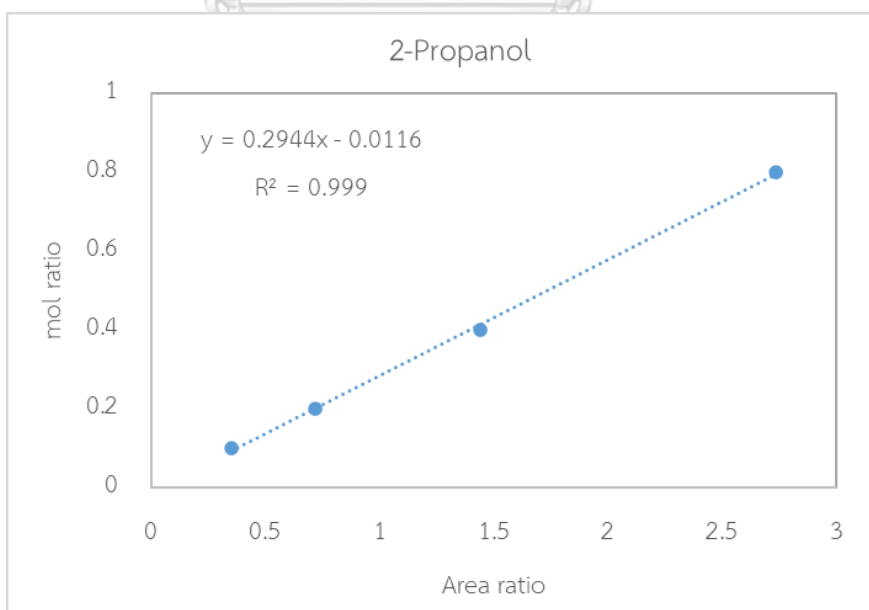
APPENDIX A

CALIBRATION CURVES

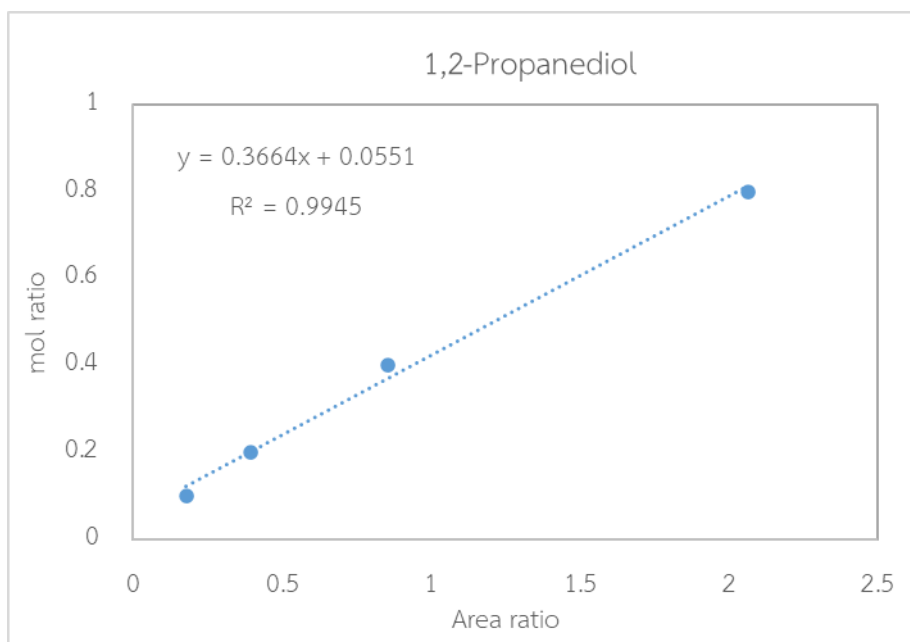
Calibration of products analyzed by GC technique



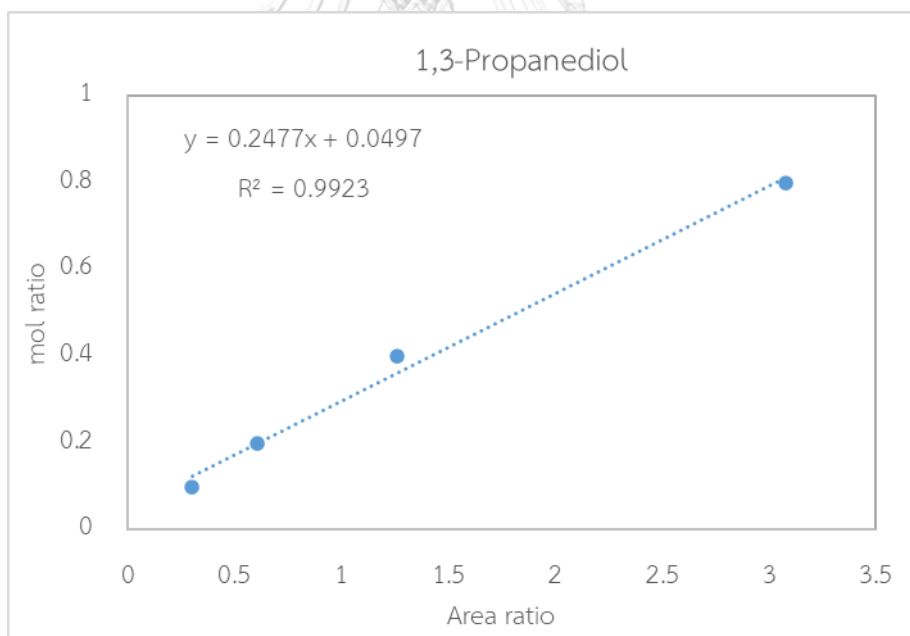
Calibration curve of 1-Propanol



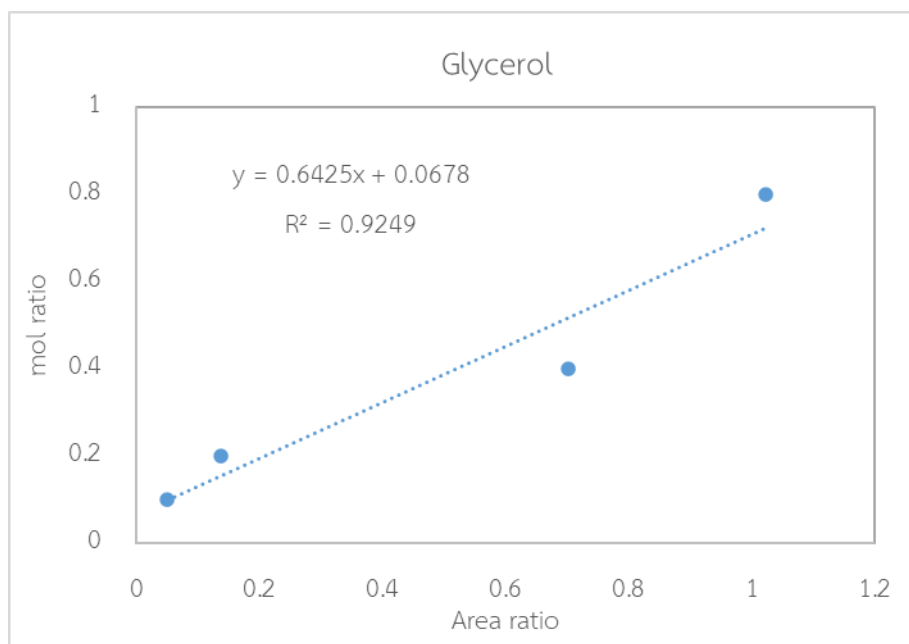
Calibration curve of 2-Propanol



Calibration curve of 1,2-Propanediol



Calibration curve of 1,3-Propanediol



Calibration curve of glycerol



APPENDIX B CALCULATIONS

B.1 Catalyst preparation

Precursor information

- Ammonium (Meta) tungstate $(\text{NH}_4)_6\text{H}_2\text{W}_{12}\text{O}_{40} \cdot n\text{H}_2\text{O} = 2956.3 \text{ g/mol}$ (99.99%)
- Chloroplatinic acid hydrate $\text{H}_2\text{PtCl}_6 = 409.81 \text{ g/mol}$ (38% Pt basis)
- Ammonium perrhenate $\text{NH}_4\text{ReO}_4 = 270.17 \text{ g/mol}$ (38% Pt basis)
- Rhodium (III) chloride $\text{RhCl}_3 = 209.26 \text{ g/mol}$ (38% Rh basis)
- Niobium(V) chloride $\text{NbCl}_5 = 270.17 \text{ g/mol}$ (99% Nb basis)
- Tungstosilicic acid hydrate $\text{H}_4(\text{W}_{12}\text{SiO}_{40}) = 2870.16 \text{ g/mol}$

Preparation platinum stock

1g of Chloroplatinic acid hydrate H_2PtCl_6 was dissolved in 15ml of DI water

Preparation 5%Pt/ $\text{WO}_x/\text{Al}_2\text{O}_3$ catalyst

Based on 100 g of catalyst amount

Pt metal (Pt) = 5 g

$\text{WO}_x/\text{Al}_2\text{O}_3$ catalyst = 95 g

Required amount 2 g catalyst = Pt metal (Pt) = $\frac{5}{95} \times 2 = 0.1053 \text{ g}_{\text{Pt}}$

So; $0.1053 \text{ g}_{\text{Pt}} \times \frac{15\text{ml}}{\text{Pt}1\text{g}} \times \frac{100\text{g}}{\text{Pt}38\text{g}} = 4.157\text{ml}$

B.2 CO-Chemisorption

$$V_{\text{ads}} = \frac{V_{\text{inj}}}{m} \times \sum_{i=1}^n \left(1 - \frac{A_i}{A_f}\right)$$

$$\text{Metal Active Site} = S_f \frac{V_{\text{ads}}}{22414} \times 10^{-6} \mu\text{mol/g}_{\text{cat.}}$$

$$d = \frac{F_g}{\rho \times \text{MSA}_m} \times \frac{\text{m}^3}{10^6 \text{m}^3} \times \frac{10^9 \text{nm}}{\text{m}}$$

$$\%D = S_f \frac{V_{\text{ads}}}{V_g} \times \frac{\text{m. w.}}{\%M} \times 100\% \times 100\%$$

Calculation by CO-Chemisorption technique

Catalyst amount = 0.1 g

Injected volume = 0.02 μL

i	Area	$1-A_i/A_f$	V_{ads}^i	sum V_{ads}^i
1	0.02448	0.363495	0.072698908	0.072699
2	0.02301	0.401716	0.080343214	0.153042
3	0.02274	0.408736	0.08174727	0.234789
4	0.02313	0.398596	0.079719189	0.314509
5	0.0229	0.404576	0.080915237	0.395424
6	0.02329	0.394436	0.078887155	0.474311
7	0.02457	0.361154	0.072230889	0.546542
8	0.02648	0.311492	0.062298492	0.60884
9	0.02787	0.275351	0.055070203	0.663911
10	0.03256	0.153406	0.030681227	0.694592
11	0.03631	0.055902	0.011180447	0.705772
12	0.03884	0.705772231		cm ³ /g
13	0.03857			
14	0.03797			
A_f	0.03846			

i = Order of injection

Area = Result from monitor

A_i = Area at i

A_f = Average of the area at 12, 13, and 14 or the saturated area

$$A_f = \left(\frac{0.03884 + 0.03857 + 0.03797}{3} \right) = 0.705772$$

$$V_{\text{ads}}^i = \frac{0.02 \text{ cm}^3}{0.1 \text{ g}} \times 0.363495 = 0.072699 \text{ cm}^3/\text{g}$$

$$V_{ads} = \sum V_{ads}^i = 0.705772 \text{ cm}^3/\text{g}$$

$$\text{Surface Area} = 1 \times \frac{0.705772}{22414} \times \frac{100}{5} \times 6.023 \times 10^{23} \times 0.08 \times \frac{1}{10^{18}} = 30.34 \text{ m}^2/\text{g}$$

$$\% \text{Dispersion} = 1 \times \frac{0.705772}{22414} \times \frac{195.078}{5} \times 100\% \times 100\% = 12.3\%$$

$$\text{Metal Size} = \frac{6}{21.09 \times 30.34} \times \frac{10^9}{10^6} = 9.38 \text{ nm}$$

B.3 Metal size calculation by XRD technique

Fresh-Pt/WO _x /Al ₂ O ₃		Used-Pt/WO _x /Al ₂ O ₃	
FWHM	Position	FWHM	Position
1.23	39.528	1.10	39.814
0.9 × λ	0.139	0.9 × λ	0.139
FWHM (radian)	0.021	FWHM (radian)	0.019
Theta/2	19.764	Theta/2	19.907
cos(radian)	0.610	cos(radian)	0.491
Metal size (nm)	10.616	Metal size (nm)	14.673

From Scherrer equation

$$\text{Metal Size} = \frac{k\lambda}{\beta \cos\theta}$$

- Pt metal size of Fresh-Pt/WO_x/Al₂O₃ catalyst

$$\text{Metal Size} = \frac{0.9 \times 0.15406}{0.021 \times \cos(19.764)} = 10.616 \text{ nm}$$

- Pt metal size of Fresh-Pt/WO_x/Al₂O₃ catalyst

$$\text{Metal Size} = \frac{0.9 \times 0.15406}{0.019 \times \cos(19.907)} = 14.673 \text{ nm}$$

B.4 Metal leaching calculation by ICP-EOS technique

The result from ICE-EOS analysis

- Pt leaching

Catalyst	ICP Detection
5Pt/WO _x /Al ₂ O ₃	0.002
0.1Rh/5Pt/WO _x /Al ₂ O ₃	-0.014
0.1Nb/5Pt/WO _x /Al ₂ O ₃	0.0045
0.1Re/5Pt/WO _x /Al ₂ O ₃	-0.019
0.1HSiW/5Pt/WO _x /Al ₂ O ₃	-0.744

Catalyst	Pt leaching
5Pt/WO _x /Al ₂ O ₃	0.00002392
0.1Rh/5Pt/WO _x /Al ₂ O ₃	-0.00016746
0.1Nb/5Pt/WO _x /Al ₂ O ₃	0.00005383
0.1Re/5Pt/WO _x /Al ₂ O ₃	-0.00022727
0.1HSiW/5Pt/WO _x /Al ₂ O ₃	-0.00889928

Pt leaching (mg)

Data for calculation

$$\text{Glycerol } 0.36 \text{ g} = 0.36 \text{ g}_{\text{Gly}} / (1.11 \text{ g}_{\text{Gly}} \text{ ml}^{-1}) = 0.324 \text{ ml}$$

$$\text{Glycerol } 11.64 \text{ g} = 11.64 \text{ g}_{\text{water}} / (1 \text{ g}_{\text{water}} \text{ ml}^{-1}) = 11.64 \text{ ml}$$

$$\text{Initial volume} = (0.324 + 11.64) = 11.9614 \text{ ml (Glycerol and DI-water volume)}$$

$$\text{Pt leaching} = \frac{0.002 \times 11.9614}{1000} = 0.00002392 \text{ mg}$$

Initial Pt amount on the fresh catalyst

$$\text{Pt} = 5\%/100\% \times 0.6 \text{ g} = 0.03 \text{ g} = 30 \text{ mg Pt}$$

%Pt leaching in liquid phase reaction

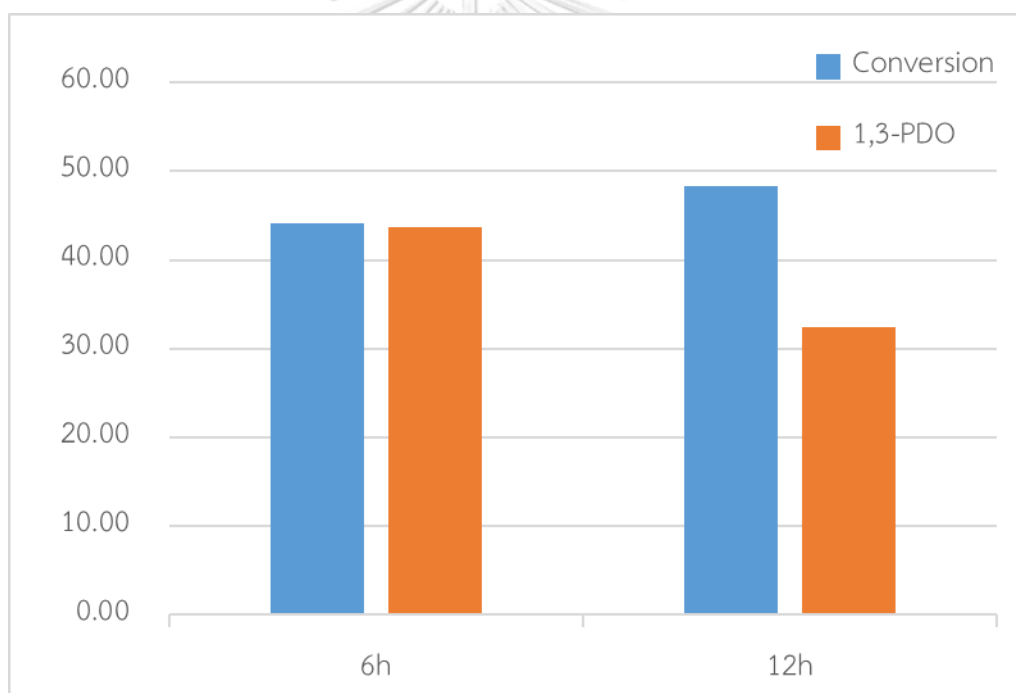
$$\% \text{Pt leaching} = \frac{0.00002392}{30} \times 100 \times 1000 = 0.8\%$$



APPENDIX C

REACTION TIME

The hydrogenolysis of glycerol during 6 h compared with 12 h as shown in the figure the results increase glycerol conversion from 44.16% to 48.27% after increase reaction time to 12 h. Additionally, the 1,3-propanediol selectivity decrease from 43.66% to 32.45%. However, decreased 1,3-propanediol selectivity can increase other by-products such as 1-propanol, 2-propanol which are the product can undergo by the series reaction. So, the reaction time for optimum 1,3-propanediol selectivity is 6 h.



Performance of catalyst on hydrogenolysis during 6 h compared with 12 h

REFERENCES

1. *Global primary energy consumption by source*. 2017; Available from: <https://ourworldindata.org/grapher/global-energy-consumption-source>.
2. Hocking, M.B., *Handbook of Chemical Technology and Pollution Control*. 2005.
3. *United States Environmental Protection Agency*. 2015; Available from: <http://www.epa.gov/climatechange/ghgemissions/global.html>.
4. Ragauskas, A.J., *The Path Forward for Biofuels.pdf*. SCIENCE, 2006. **311**.
5. H. Zhang, U.A.O., Q. Wang, Z. Zhao, *Renewable & Sustainable Energy Reviews*, 2014. **38**: p. 677-685.
6. *Biodiesel production: a review*. *Bioresource Technology*, 1999. **70**: p. 1-15.
7. *PSUBiodiesel*.
8. Fangxia Yang, M.A.H.a.R.S., *Value-added uses for crude glycerol--a byproduct of biodiesel production*. *Biotechnology for Biofuels*, 2012. **5**: p. 13.
9. Sun, D., et al., *Glycerol hydrogenolysis into useful C3 chemicals*. *Applied Catalysis B: Environmental*, 2016. **193**: p. 75-92.
10. Xi, Z., et al., *Hydrogenolysis of Glycerol on the ZrO₂-TiO₂ Supported Pt-WO_x Catalyst*. *Catalysts*, 2020. **10**(3).
11. Argyle, M. and C. Bartholomew, *Heterogeneous Catalyst Deactivation and Regeneration: A Review*. *Catalysts*, 2015. **5**(1): p. 145-269.
12. Sandra Imaculada Maintinguer, R.R.H.a.J.E.d.O., *Glycerol as a Raw Material for Hydrogen Production*. *Biofuels - Status and Perspective*, 2015.
13. S.A., S. *Solvay to build bio-based epichlorohydrin plant in China to serve largest market in the world*. 2012; Available from: <http://www.solvay.com>.
14. Dufey, A., *Biofuels Production, Trade and Sustainable Development: Emerging Issues*. 2006.
15. Mosser-Ruck, R., et al., *Effects of ethylene glycol saturation protocols on XRD patterns: a critical review and discussion*. *clays and clay minerals*, 2005. **53**(6): p. 631-638.
16. Nakagawa, Y. and K. Tomishige, *Heterogeneous catalysis of the glycerol hydrogenolysis*. *Catalysis Science & Technology*, 2011. **1**(2).

17. LibreTexts, C. *Hydrogenolysis*. 2019; Available from: <https://chem.libretexts.org>.
18. Fangxia Yang, M.A.H.a.R.S., *Value-added uses for crude glycerol--a byproduct of biodiesel production*. *Biotechnology for Biofuels*, 2012 **5**: p. 13.
19. Samudrala, S.P., S. Kandasamy, and S. Bhattacharya, *Turning Biodiesel Waste Glycerol into 1,3-Propanediol: Catalytic Performance of Sulphuric acid-Activated Montmorillonite Supported Platinum Catalysts in Glycerol Hydrogenolysis*. *Sci Rep*, 2018. **8**(1): p. 7484.
20. M. Pagliaro, M.R., *The Future of Glycerol*. The Royal Society of Chemistry, 2008.
21. Sorona, D. *NEW INVESTMENT TO MEET THE GROWING DEMAND FOR BIOMATERIALS*. 2018; Available from: <http://sorona.com/article/duPont-tate-lyle-bio-products-expanding-bio-based-propanediol-production-in-tennessee/>.
22. Jan, J.G. *Enzyme Technology* Available from: BiologyMad.com.
23. Gu, M., et al., *Selective Hydrogenolysis of Erythritol over Ir-ReO_x /Rutile-TiO₂ Catalyst*. *ChemSusChem*, 2020.
24. Bartholomew, C.H., *Carbon Deposition in Steam Reforming and Methanation*. *Catalysis Reviews*, 1982. **24**(1): p. 67-112.
25. Besson, M. and P. Gallezot, *Deactivation of metal catalysts in liquid phase organic reactions*. *Catalysis Today*, 2003. **81**(4): p. 547-559.
26. Goodman, J.A.R.a.D.W., *The Nature of the Metal-Metal Bond in Bimetallic Surfaces*. *Science, New Series*, 1992. **257**: p. 897-903.
27. Dasari, M.A., et al., *Low-pressure hydrogenolysis of glycerol to propylene glycol*. *Applied Catalysis A: General*, 2005. **281**(1-2): p. 225-231.
28. Miyazawa, T., et al., *Development of a Ru/C catalyst for glycerol hydrogenolysis in combination with an ion-exchange resin*. *Applied Catalysis A: General*, 2007. **318**: p. 244-251.
29. Cai, F., et al., *Hydrogenolysis of glycerol over supported bimetallic Ni/Cu catalysts with and without external hydrogen addition in a fixed-bed flow reactor*. *Applied Catalysis A: General*, 2018. **564**: p. 172-182.
30. Wang, J., et al., *Hydrogenolysis of Glycerol to 1,3-propanediol under Low Hydrogen Pressure over WO_x -Supported Single/Pseudo-Single Atom Pt Catalyst*. *ChemSusChem*, 2016. **9**(8): p. 784-90.

31. Liu, L., et al., *Mesoporous WO₃ Supported Pt Catalyst for Hydrogenolysis of Glycerol to 1,3-Propanediol*. Chinese Journal of Catalysis, 2012. **33**(7-8): p. 1257-1261.
32. Arundhathi, R., et al., *Highly selective hydrogenolysis of glycerol to 1,3-propanediol over a boehmite-supported platinum/tungsten catalyst*. ChemSusChem, 2013. **6**(8): p. 1345-7.
33. Mizugaki, T., et al., *Selective Hydrogenolysis of Glycerol to 1,3-Propanediol Catalyzed by Pt Nanoparticles–AlO_x/WO₃*. Chemistry Letters, 2012. **41**(12): p. 1720-1722.
34. García-Fernández, S., et al., *New approaches to the Pt/WO₃/Al₂O₃ catalytic system behavior for the selective glycerol hydrogenolysis to 1,3-propanediol*. Journal of Catalysis, 2015. **323**: p. 65-75.
35. Kurosaka, T., et al., *Production of 1,3-propanediol by hydrogenolysis of glycerol catalyzed by Pt/WO₃/ZrO₂*. Catalysis Communications, 2008. **9**(6): p. 1360-1363.
36. Qin, L.-Z., M.-J. Song, and C.-L. Chen, *Aqueous-phase deoxygenation of glycerol to 1,3-propanediol over Pt/WO₃/ZrO₂ catalysts in a fixed-bed reactor*. Green Chemistry, 2010. **12**(8).
37. Zhu, S., et al., *SiO₂ promoted Pt/WO_x/ZrO₂ catalysts for the selective hydrogenolysis of glycerol to 1,3-propanediol*. Applied Catalysis B: Environmental, 2014. **158-159**: p. 391-399.
38. Zhou, W., et al., *WO_x domain size, acid properties and mechanistic aspects of glycerol hydrogenolysis over Pt/WO_x/ZrO₂*. Applied Catalysis B: Environmental, 2019. **242**: p. 410-421.
39. Lei, N., et al., *Understanding the deactivation behavior of Pt/WO₃/Al₂O₃ catalyst in the glycerol hydrogenolysis reaction*. Chinese Journal of Catalysis, 2020. **41**(8): p. 1261-1267.
40. Saelee, T., et al., *Experimental and computational study on roles of WO_x promoting strong metal support promoter interaction in Pt catalysts during glycerol hydrogenolysis*. Scientific Reports, 2021. **11**(1).
41. Wang, J., et al., *Effect of promoters on the selective hydrogenolysis of glycerol over Pt/W-containing catalysts*. Chinese Journal of Catalysis, 2016. **37**(9): p.

- 1513-1519.
42. Huo, J., et al., *Deactivation and regeneration of carbon supported Pt and Ru catalysts in aqueous phase hydrogenation of 2-pentanone*. Catalysis Science & Technology, 2020. **10**(9): p. 3047-3056.
 43. García-Fernández, S., et al., *Influence of the Support of Bimetallic Platinum Tungstate Catalysts on 1,3-Propanediol Formation from Glycerol*. ChemCatChem, 2017. **9**(24): p. 4508-4519.
 44. Li, W., et al., *Platinum dendritic nanoparticles with magnetic behavior*. Journal of Applied Physics, 2014. **116**(3).
 45. Nguyen, V.-L., et al., *Structure and morphology of platinum nanoparticles with critical new issues of low- and high-index facets*. Advances in Natural Sciences: Nanoscience and Nanotechnology, 2012. **3**(2).
 46. Edake, M., et al., *Catalytic glycerol hydrogenolysis to 1,3-propanediol in a gas-solid fluidized bed*. RSC Advances, 2017. **7**(7): p. 3853-3860.
 47. Zhu, S., et al., *Promoting effect of WO_x on selective hydrogenolysis of glycerol to 1,3-propanediol over bifunctional Pt-WO_x/Al₂O₃ catalysts*. Journal of Molecular Catalysis A: Chemical, 2015. **398**: p. 391-398.
 48. Iwashita, N., *X-ray Powder Diffraction*, in *Materials Science and Engineering of Carbon*. 2016. p. 7-25.
 49. Daniel, O.M., et al., *X-ray Absorption Spectroscopy of Bimetallic Pt-Re Catalysts for Hydrogenolysis of Glycerol to Propanediols*. ChemCatChem, 2010. **2**(9): p. 1107-1114.
 50. Fan, Y., et al., *Pt-WO on monoclinic or tetrahedral ZrO₂: Crystal phase effect of zirconia on glycerol hydrogenolysis to 1,3-propanediol*. Applied Catalysis B: Environmental, 2017. **217**: p. 331-341.
 51. Zhou, C.-H., et al., *Chemoselective catalytic conversion of glycerol as a biorenewable source to valuable commodity chemicals*. Chemical Society Reviews, 2008. **37**(3): p. 527-549.



จุฬาลงกรณ์มหาวิทยาลัย
CHULALONGKORN UNIVERSITY

VITA

NAME Therasak Tapanya

DATE OF BIRTH 1 January 1997

PLACE OF BIRTH Saraburi

HOME ADDRESS 38 Village No.7 Sutbuntad Road, Tandew Sub-district,
Kaeng Khoi District, Saraburi, 18110

